CHAPTER 3

RESULTS AND DISCUSSION

3.1 Comparison of the designed flow-through cell to the commercial flow-through cell.

This thesis was carried out through the designed flow-through cell in conjugation with the flow injection system. The characteristic of the sample peak was investigated by injecting 75 uL of 30 ppm standard iron solution into the carrier stream (0.2% neutralized thioglycolic acid in 0.3 M ammonia solution) at the flow rate of 4.0 mL min^{-1} by means of a 100 uL microsyringe, via an injection port through the mixing coil of length 150 cm (diameter 1.0 mm i.d.). The sample peak, as shown in Figure 3.1, was recorded at 535 nm by measuring the absorbance versus time. The similar experiment was then repeated with the commercially available Beckman 75 uL flow-through cell and the sample peak was also shown in Figure 3.1. The results of these experiments showed that the sensitivity (peak height) of the designed flow-through cell is slightly lower than that of the commercial one. The reason for this effect was that the internal volume of the designed flow-through cell was 5 uL larger and therefore the dispersion of sample zone would also become larger than that of the commercial flow-through cell. The falling curve of the designed flow-through cell was smooth and its tailing was short like the commercial flow-through cell. The residence time of system using the commercial and the designed flow-through cell was 40 s and 36 s

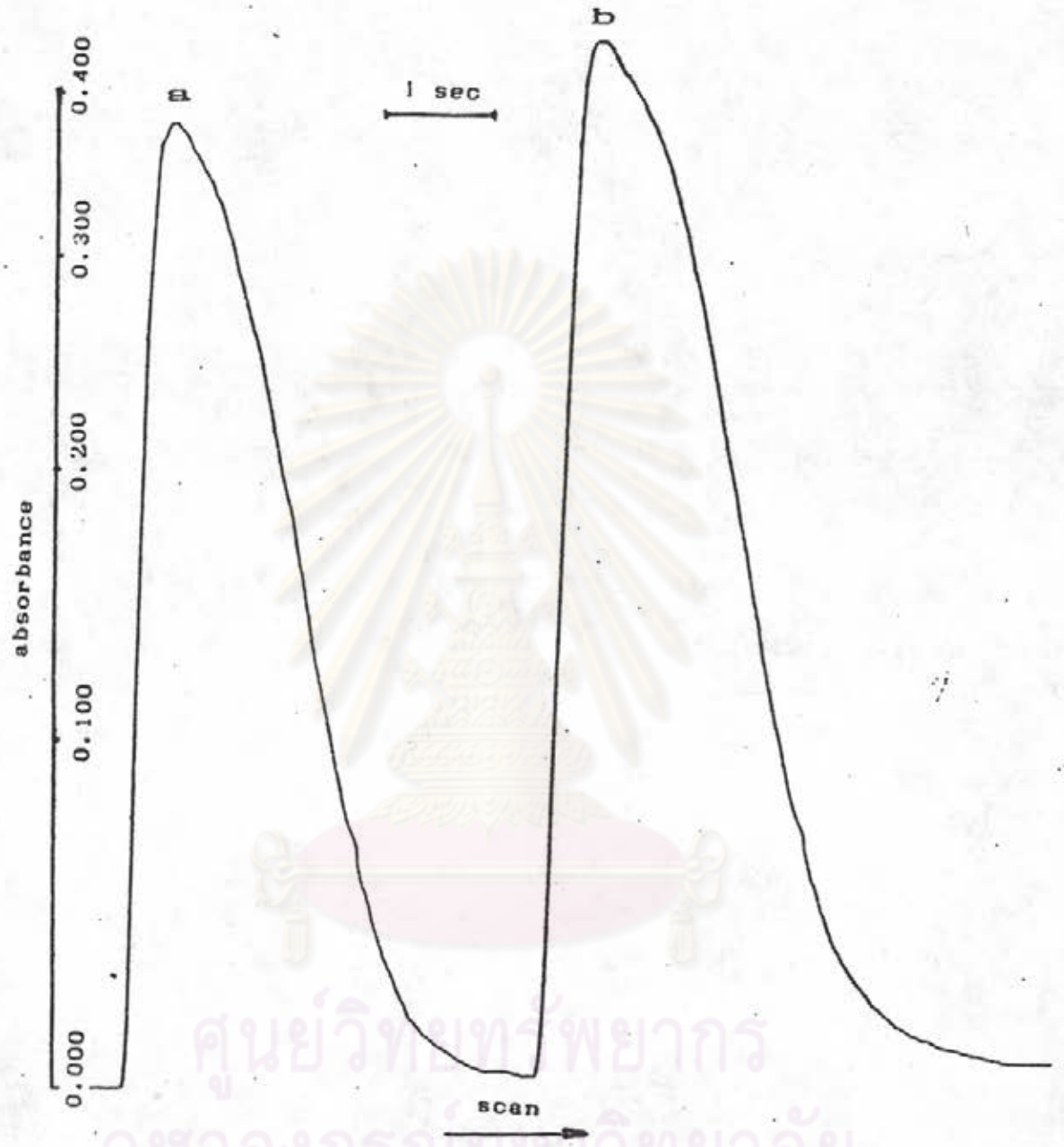

Figure 3.1 The sample peak of the designed flow-through cell (a) and the commercial flow-through cell (b) by injecting 75 uL of 30 ppm iron solution into thioglycolate reagent carrier stream at the flow rate of 4.0 mL min^{-1}.

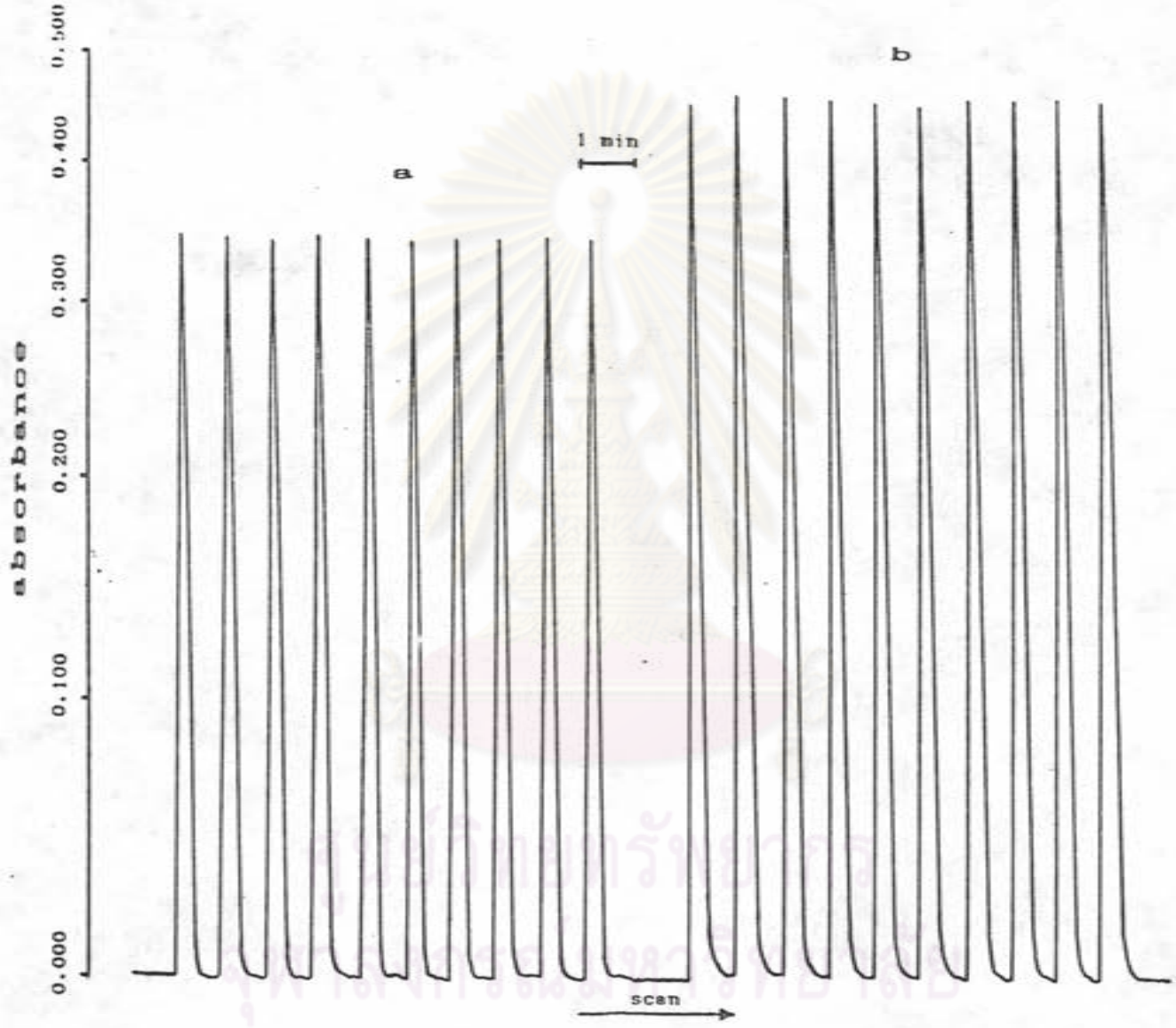

Figure 3.2 The sample peak for 10 replicates of the designed flow-through cell (a) and the commercial flow-through cell (b) by injecting 75 uL of 30 ppm standard iron solution into the thioglycolate reagent at the flow rate of 4.0 mL min^{-1}.

respectively. The peak height for 10 replicates of both designed and commercial flow-through cell at chart speed of 10 mm min^{-1} was shown in Figure 3.2. It can be seen that the reproducibility of the peaks when employing the designed flow-through cell is better than that of the commercial one, 0.44 RSD for the first and 0.68 RSD for the later.

From these studies, it shows that the designed flow-through cell can be employed in the flow injection system as well as the commercial flow-through cell.

3.2 Determination of Alumina

3.2.1 Optimization studies on the Al-alizarin red S complex in batch analysis

In order to achieve the best condition for flow analysis, various factors including maximum wavelength, rate of reaction, pH, temperature of solution and interfering ions, must be studied to optimize the condition.

The use of alizarin as a colorimetric reagent for aluminium determination was suggested by Attack (47). The difference in color of the aluminium complex with alizarin and the reagent itself permits the colorimetric determination of aluminium in acid solution. However, owing to its low solubility in water, the reagant was not used for any extent, and alizarin red S (sodium alizarinsulfonate) was employed instead, to get more solubility.

Figure 3.3 shows the spectra of alizarin red S and Al-alizarin red S complex solution measured against a water blank solution. The maximum absorbance of alizarin red S was at 422 nm and that of Al-alizarin red S complex was at 480 nm. These results agreed with the work done by Parker and Goddard (48).

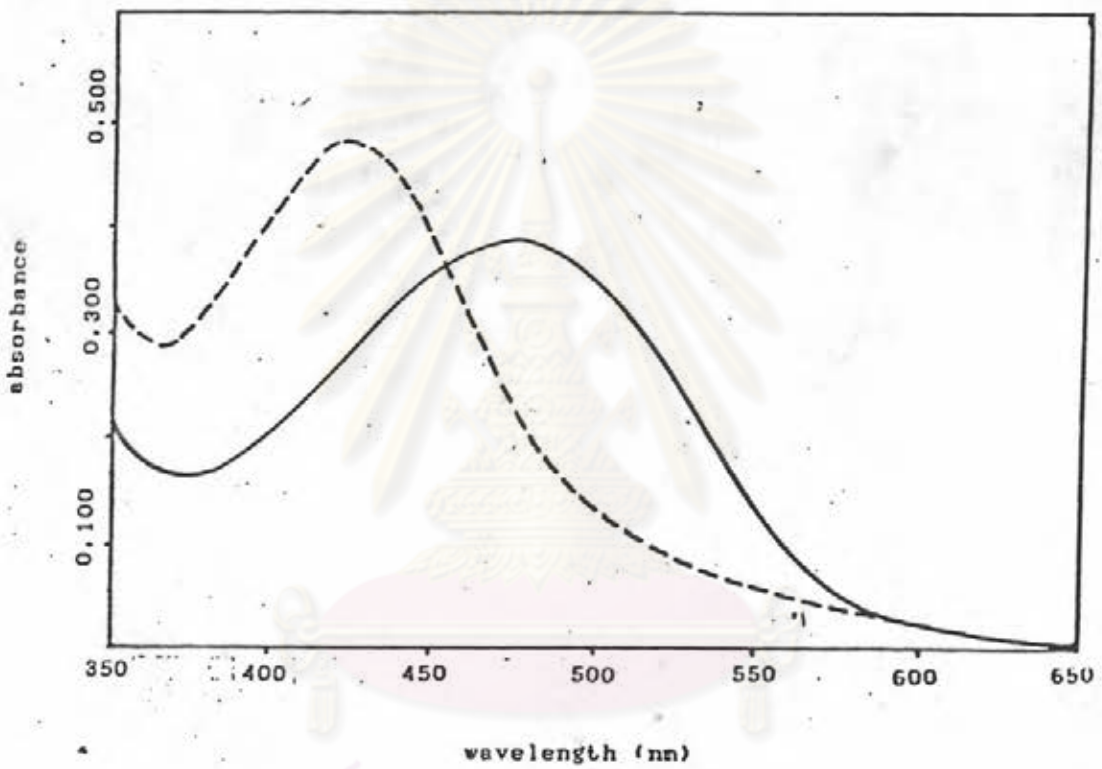

Figure 3.3 Absorption spectra of alizarin red S and its aluminium complex; (- -), 0.01% alizarin red S at pH 4.5: (——), 50 ug of aluminium in 50 mL of 0.1%alizarin red S.

Effect of pH on the maximum absorption and sensitivity of this complex was studied by varying the pH of ammonium acetate buffer solution. The results in Figure 3.4 show that the absorption band of complex shifts toward the red at higher pH. At pH 5.0, the

absorption peak was broad and the sensitivity at the maximum absorbance was the lowest. To achieve the highest sensitivity, the absorption ratio of the complex to reagent should be at the maximum value. It was found that the highest sensitivity can be obtained by adjusting the solution to pH 4.5 and measuring at 510 nm. This condition was therefore, used for all aluminium analyses in this thesis.

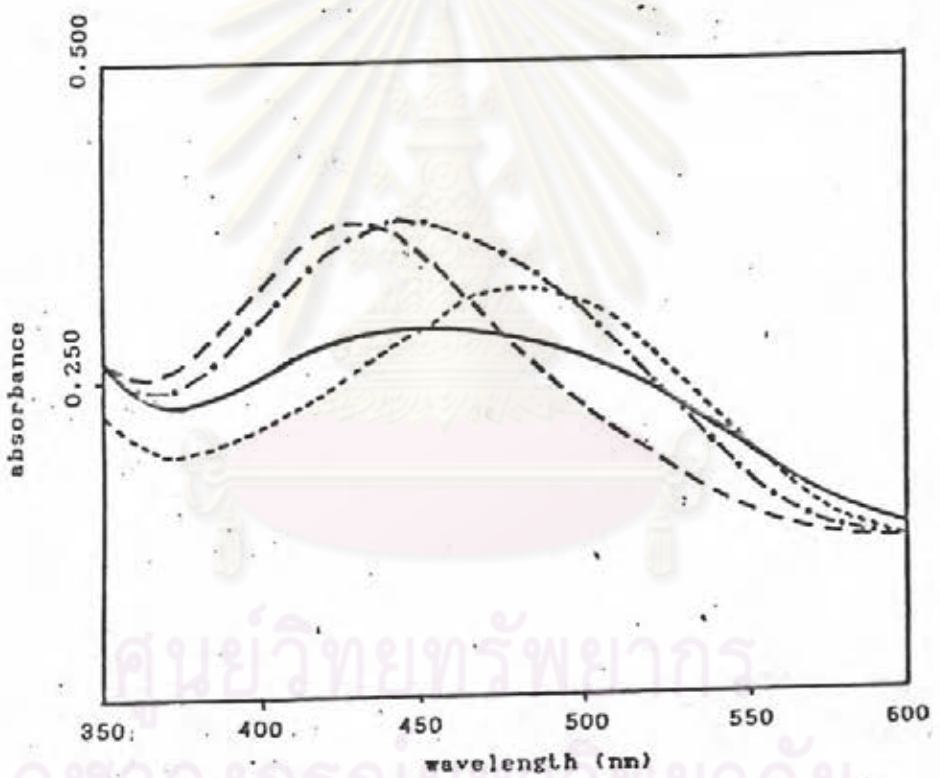

Figure 3.4 Effect of pH on the absorption spectra of the aluminium complex (50 ug of aluminium in 50 mL of 0.01 % alizarin red S solution); (- - -), pH3.5; (-·-·), pH 4.0; (-·-·), pH 4.5; (——),pH 5.0.

However, pH of buffer solution not only shifts the absorption band, but also has affect on the rate of complex formation. Effect of pH on time for color development is shown in Figure 3.5. The shortest time for the color development was 4 min at pH 4.5 of the buffer solution. Figure 3.6 shows the time needed for the color development at the temperature of 25°C and 60°C. At the temperature of 25°C, the color development took about 5 min to be completed. When the solution was heated to 60 °C, the color developed faster. It took about 2 min for the reaction to get completed. These results

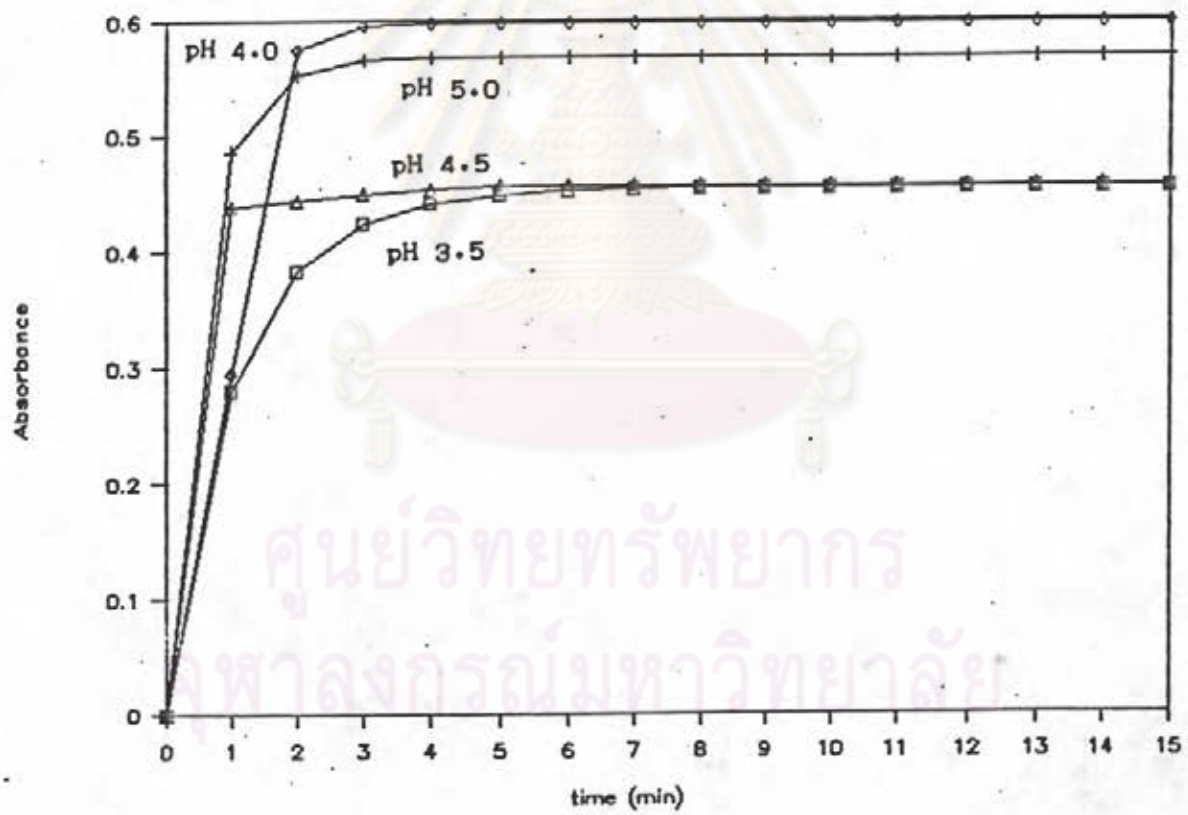

Figure 3.5 Effect of pH on the rate of complex formation of 6.0 ug/L of aluminium in 0.01% alizarin red S in ammonium acetate buffer solution.

showed that the pH 4.5 and temperature of 60°C (of buffer solution) should be employed to obtained the optimum condition for the determination of aluminium.

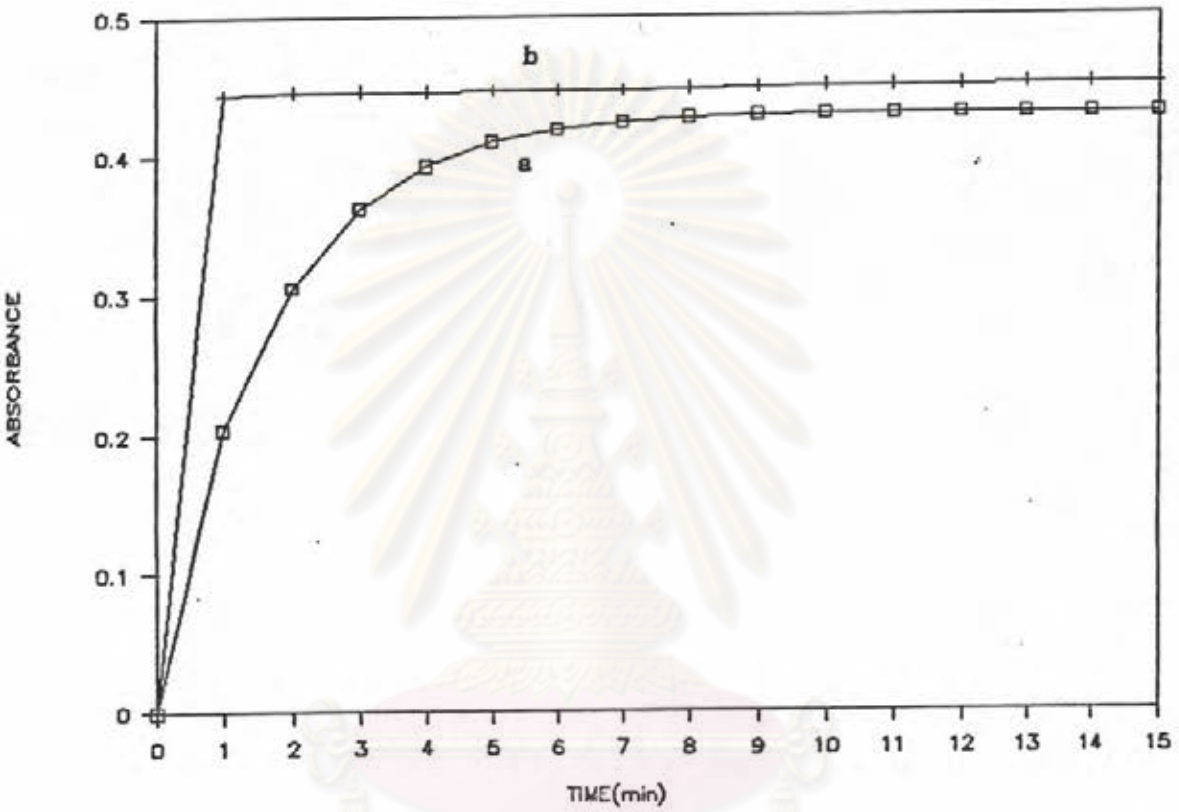

Figure 3.6 Effect of temperature on the rate of complex formation of 6.0 ug/L aluminium and 0.01 % alizarin red S in ammonium acetate buffer solution (pH 4.5) at 25°C (a) and 60 °C (b).

Besides aluminium, elements normally presented in kaolins and lateritic soils, are silicon, iron, calcium, magnesium, titanium, potassium, sodium, manganese, etc.. Calcium and iron (49) were reported to give marked effect on the determination of aluminium when alizarin red S was employed.

In the presence of calcium, the color of aluminium complex was intensified and the absorption band shifted toward the red. The effect of calcium on the absorption spectrum of the reagent was insignificant in the absence of aluminium. When the amount of calcium was increased from 160 mg/L, the color intensity remained constant, and at the amount more than 300 mg/L, the solution became turbid. Thus, in this work the amount of calcium in the reagent solution used to protect the intensified color due to calcium ion interference in the sample was 200 mg/L.

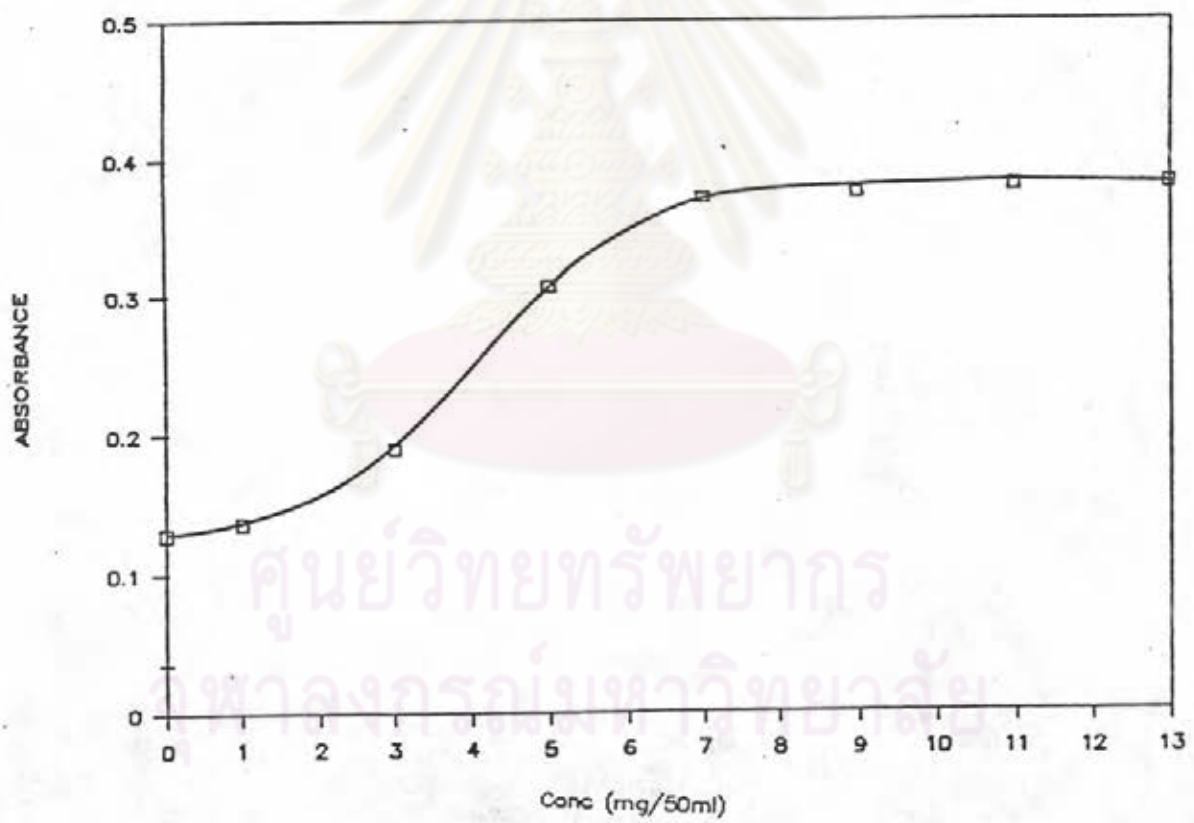

Figure 3.7 Effect of calcium on the complex formation of 0.01% alizarin red S and 1 ug/mL of aluminium in ammonium acetate buffer solution (pH 4.5).

An effort to prevent iron interference on the aluminium determination by using sodium thiosulfate and thioglycolic acid as masking agent were made and the results were given in the Table 3.1 and Table 3.2, respectively. Table 3.1 shows that sodium thiosulfate has effect on the reagent solution as it induced the color of the reagent. Thioglycolic acid as indicated in Table 3.2 has no effect on the reagent solution and also can illuminate iron interference in aluminium analysis. At the concentration of 0.04 % thioglycolic acid, the recovery of aluminium (40.0%) has found to be 38.64 % in the presence and in the absence of iron. Therefore, thioglycolic acid at the concentration of 0.04 % was used for masking the effect of iron in sample solution.

Table 3.1 Effectiveness of sodium thiosulfate as an inhibitor for iron interference when added to samples in Al analysis.

Al presented ug per 50 mL	Fe added ug per 50 mL	$Na_2S_2O_3$ added mg per 50 mL	Al found ug per 50 mL
40.00	-	-	40.00
40.00	80.00	-	62.80
40.00	-	0.10	39.00
40.00	-	0.15	43.20
40.00	-	0.20	48.20
40.00	80.00	0.10	38.60
40.00	80.00	0.15	43.20
40.00	80.00	0.20	50.00

Table 3.2 Effectiveness of thioglycolic acid as an inhibitor for iron interference when added to samples in Al analysis.

Al presented ug per 50 mL	Fe added ug per 50 mL	thioglycolic added % v/v	Al found ug per 50 mL
40.00	-	-	40.00
40.00	80.00	-	66.61
40.00	-	0.02	37.96
40.00	-	0.04	38.64
40.00	-	0.08	37.51
40.00	80.00	0.02	39.54
40.00	80.00	0.04	38.64
40.00	80.00	0.08	37.73

3.2.2 Optimization of Experimental Parameters in the Flow Injection Analysis.

In order to achieve the maximum sensitivity and the rate of sample processing, the dispersion (defined as the ratio of concentrations before and after the dispersion process taking place in the element of fluid that yields the analytical read-out) of sample in the analytical stream is one of the most important parameters in flow injection analysis. The dispersion controls the sensitivity, the rate of sampling and the precision of each flow injection procedure. The dispersion can be changed by adjusting the

injected sample volume, the flow rate of the carrier stream, the residence time and the diameter of reaction coils. Therefore, the studies of these parameters that have effect on the dispersion should be done to optimize the flow injection system.

3.2.2.1 Effect of flow rate

Effect of flow rate was investigated by injecting 100 uL of 50 ppm standard aluminium solution into the flow injection system at various flow rates. The length of mixing coil of 1.0 mm i.d. was 100 cm and 0.1 mg/mL of alizarin red S in an ammonia-acetic acid buffer solution (pH 4.50) was used as carrier stream. The recorded signal at various flow rates is shown in Figure 3.8 and the peak height is plotted against flow rates in Figure 3.9. When the total flow rate was reduced from 6.0 to 0.1 mL min^{-1}, an increase in recorded signal (peak height) was observed together with a reduction in the maximum number of sample determination per hour (increase peak width) as shown in Figure 3.8. With this analytical configuration, this result shows adverse effect to a flow injection system that is solely controlled by dispersion. At low flow rate, the sample zone stayed in analytical line for a long period of time allowing rate of complex formation to continuously proceed and also allowing the dispersion of sample zone to increase. The increase in dispersion decreased the height of sample peak while the increase in the rate of complex formation increased the height of sample peak. The total of these effect made the sample peak increased. This result indicates that the rate of complex formation is more significant than the dispersion in this condition. However, the effect of dispersion on peak tailing can still be seen on Figure 3.8 which shows that the increase in dispersion causes more peak tailing. At the flow rate of

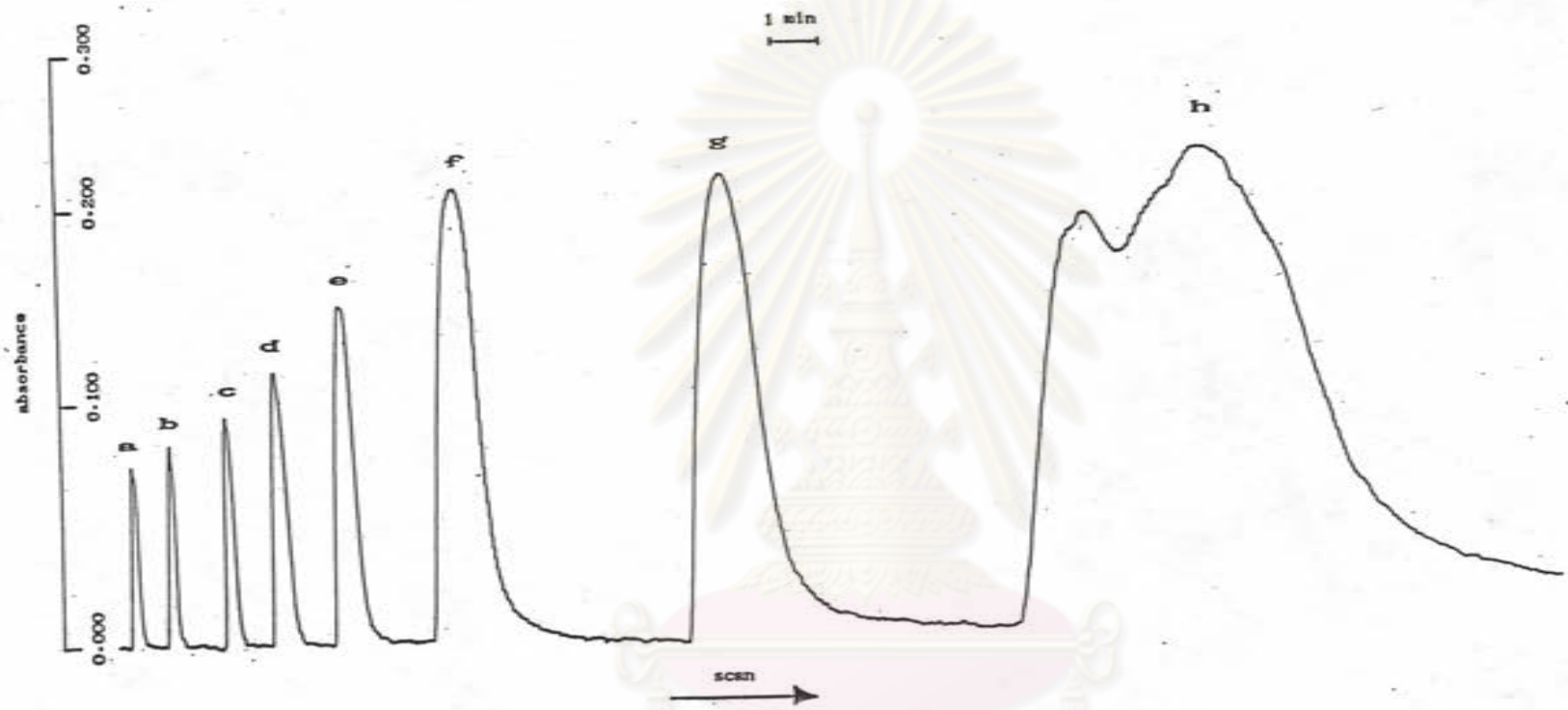

Figure 3.8 Effect of flow rate on sample peak at the following rates; (a) 6.0, (b) 5.0, (c) 4.0, (d) 3.0, (e) 2.0, (f) 1.0, (g) 0.5 and (h) 0.1 mL min^{-1} for 100 uL of 50 ppm standard aluminium solution injection by using 100 cm of 1.0 mm i.d. coil length.

0.1 mL min^{-1}, the doublet peak was obtained. The reason for this phenomena was that reagent can diffuse easily into the rear and the front of sample zone, while at the center, the reagent might not have enough time to diffuse to this point of the sample zone. Therefore, the formation of complex at the center of sample zone was limited while the formation of complex at the rear and the front went on proceeding. The result of this phenomena gives the absorbance at the center of sample zone lower than that at the rear and the front of sample zone which leads to the formation of the doublet peak. The effect of flow rate on the reproducibility of the

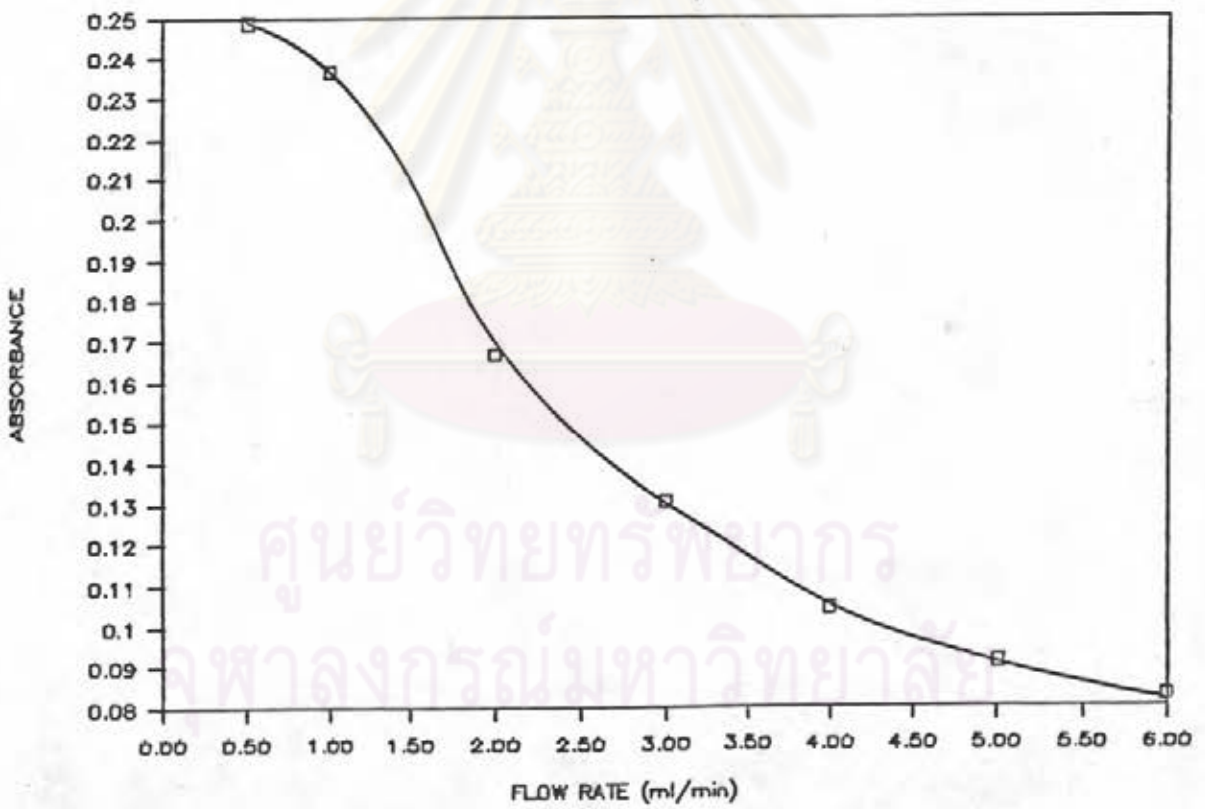

Figure 3.9 Effect of flow rate on peak heights of 50 ppm aluminium by injecting 100 uL into 0.1 % alizarin red S in ammonium acetate buffer solution (pH 4.5), coil length 100 cm, 1.0 mm i.d..

recorded signal is also shown in Table 3.3. It can be seen that the reproducibility decreased with increasing flow rate owing to the irregular pumping of carrier stream at high flow rate. The reproducibility at the flow rate in ranging from 1.0 to 5.0 mL min^{-1} are nearly equal. Thus, the flow rate of 5.0 mL min^{-1} was used to acheive the high sampling rate and sensitivity in analysis.

Table 3.3 Effect of flow rate on recorded signal, peak tailing and reproducibility by injecting 100 uL of 50 ppm aluminium solution into 0.10 mg/mL of alizarin red S carrier stream at pH 4.50.

Flow rate mL min^{-1}	Peak height Abs.	t_{base} min	RSD	Sample rate s/h
0.10	0.255	17.0	0.69	3
1.00	0.252	3.00	1.26	20
2.00	0.166	1.20	1.24	50
3.00	0.133	0.75	1.23	80
4.00	0.109	0.60	1.22	100
5.00	0.091	0.45	1.22	133
6.00	0.083	0.40	1.86	150

3.2.2.2 Effect of Injection Volume

A solution of aluminium (50 ppm) was injected into the flow system (flow rate of 5.0 mL min^{-1}) at various injection

volumes ranging from 10 to 250 uL. The reaction coil of the flow system was 100-cm of 1.0 mm i.d. teflon tube. The recorded signal after injection of each sample is shown in Figure 3.10 and the peak height of the recorded signal is plotted against the injection volume in Figure 3.11. It was found that the peak heights increased with increasing sample volume in the range of 10-250 uL. However, the increase in peak height was small above 75 uL injection, therefore, the injection volume of 75 uL was used in these aluminium analyses.

Table 3.4 Effect of sample injection volume on peak height and tailing by injecting 50 ppm of Al into 0.1 mg/mL of alizarin red S at pH 4.5 with 100 cm (1.00 mm.i.d.) coil at flow rate of 5.0 mL min^{-1}.

Injection volume uL	Peak height Absorbance	$t_{b\,\mathrm{sec}}$ sec
10	0.029	11.10
25	0.059	10.80
50	0.068	11.70
75	0.118	11.34
100	0.140	11.82
150	0.170	12.00
200	0.185	12.90
250	0.196	14.28

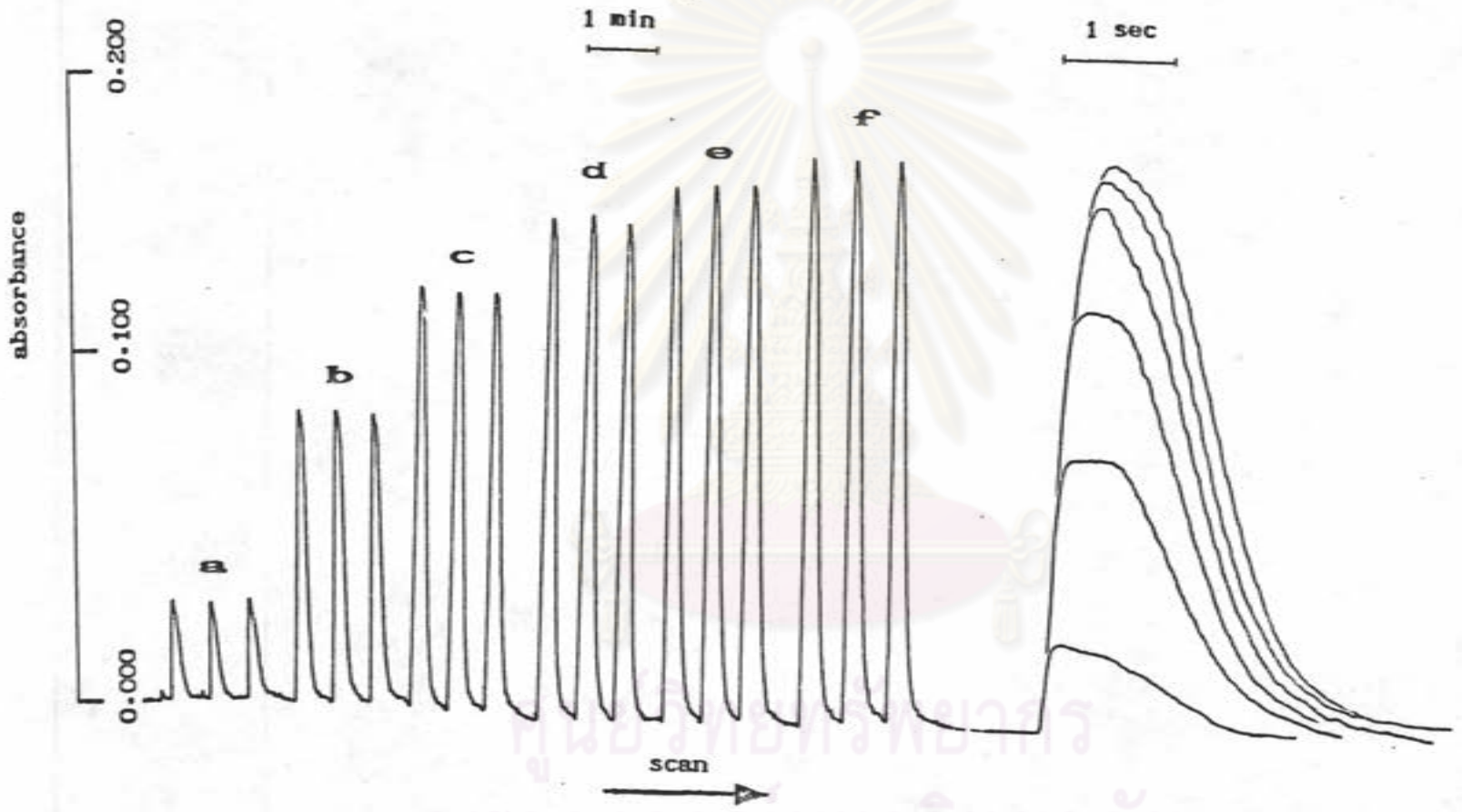

Figure 3.10 Effect of sample injection volume on sample peak at the flow rate of 5.0 mL min^{-1}: (a)10, (b)50, (c) 100, (d)150, (e)200,(f) 250, ul of 50 ppm aluminium.

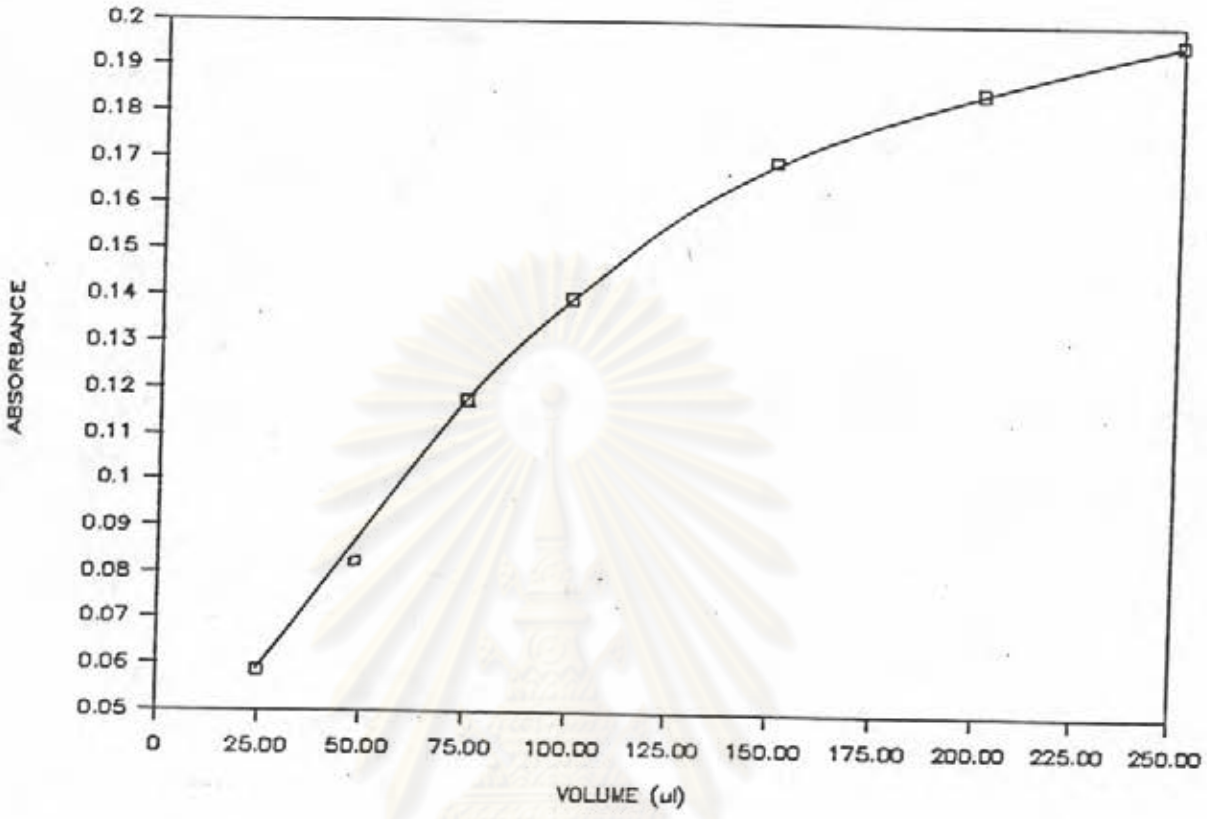

Figure 3.11 Effect of sample injection volume on peak heights for 50 ppm of aluminium at the flow rate of 5.0 mL min^{-1}.

3.2.2.3 Effect of Coil Length and Coil Diameter

Effectiveness of the residence time on the dispersion was investigated by varying the tube length between injection port and flow-through cell, and the diameter of the reaction coils. A 100 uL of aluminium solution (50 ppm) was injected into the carrier stream of 5.0 mL min^{-1} flow rate. When the length of mixing coil was varied within the range of 50-150 cm, it was found that increasing the coil length (increasing the residence time), the peak height was increased as shown on Figure 3.12 and Figure 3.13. This indicated that the formation of the

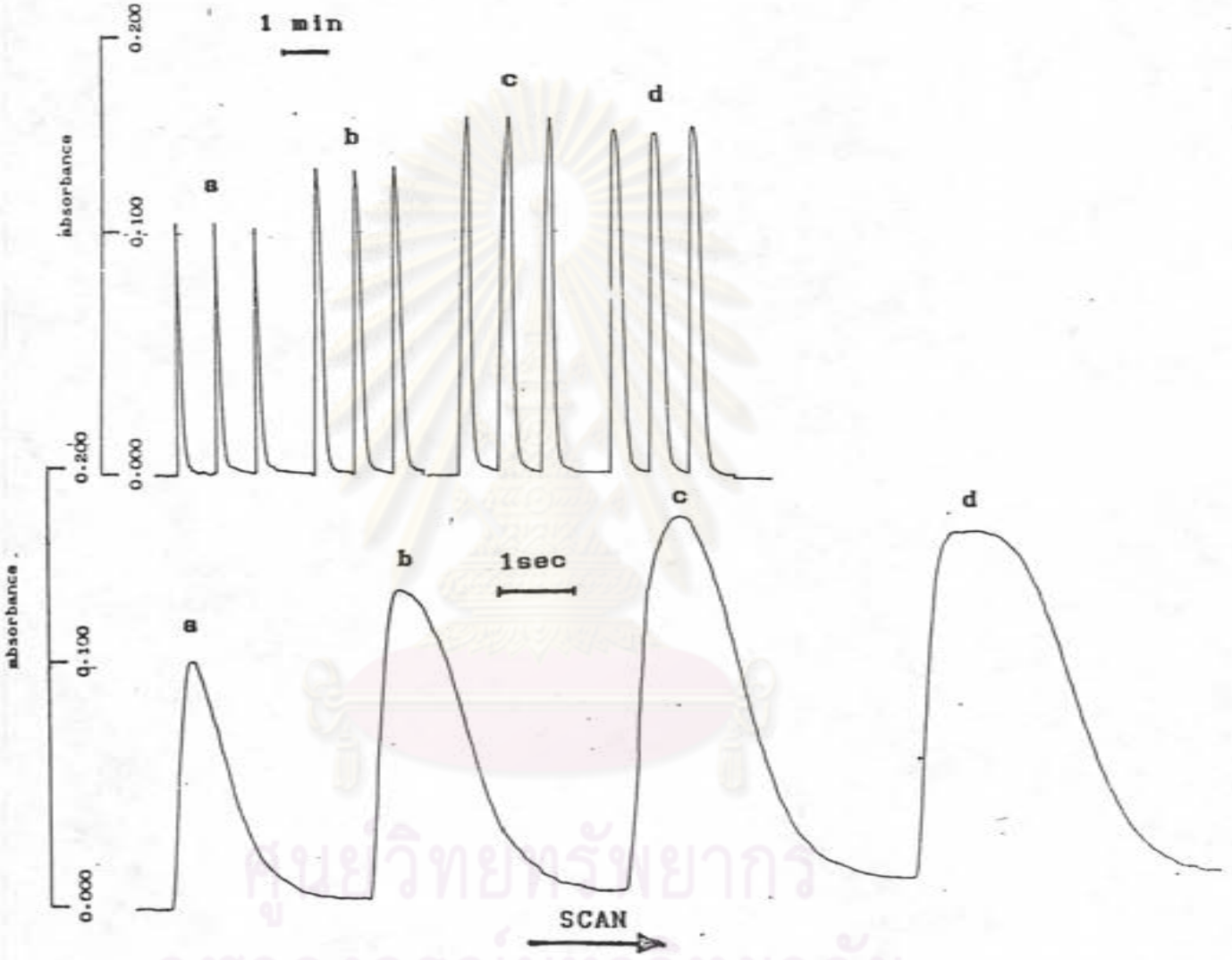

Figure 3.12 Effect of the length of 1.0 mm diameter mixing coils on sample peaks at the flow rate of 5.0 mL min^{-1}: (a)50, (b)100, (c)150, (d)200, cm for 100 ul of 50 ppm aluminium solution.

colored complex is slow and its effect on peak height is more significant than that of dispersion. However, the peak height at the coil length of 200 cm was lower than that of 150 cm. The explaination for this result is that at the coil length of 200 cm the effect of sample dispersion was more significant than that of the rate of reaction. Therefore, the coil length of 150 cm was used to acheive the highest sensitivity in the flow system.

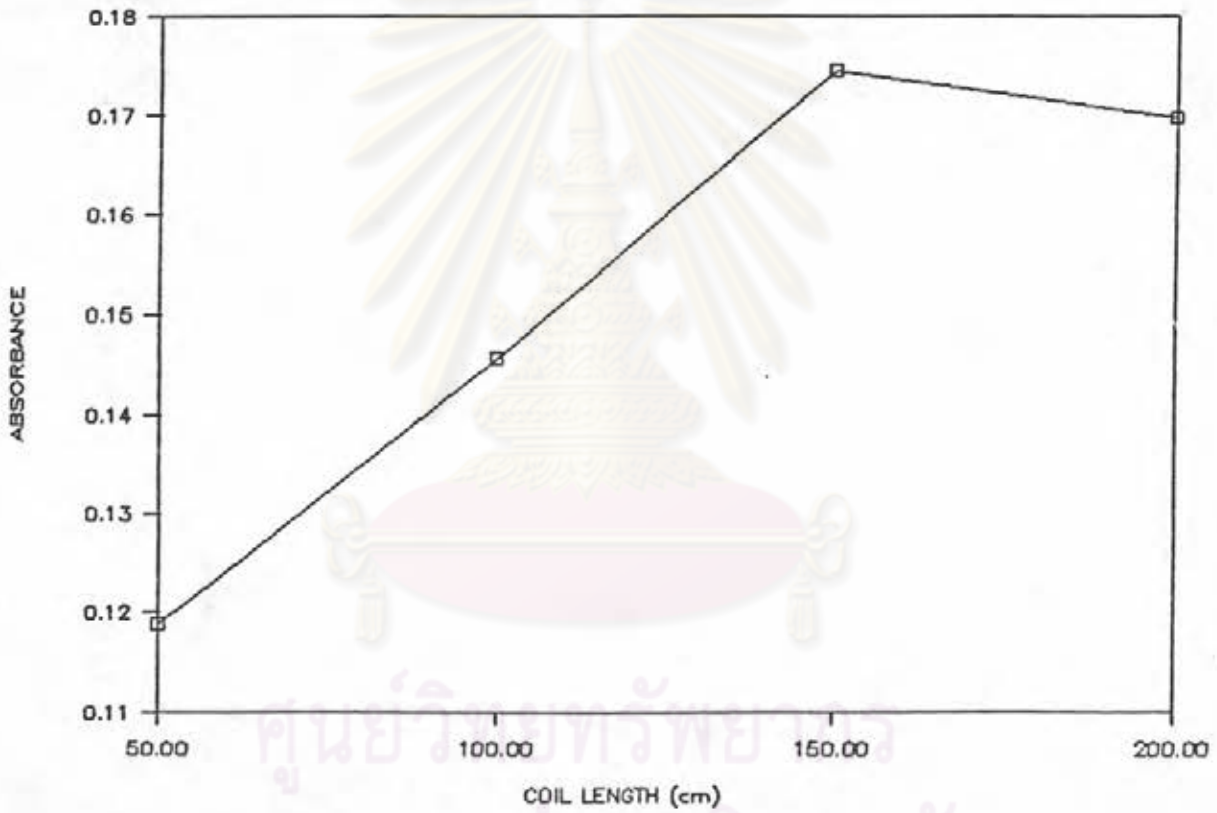

Figure 3.13 Effect of the length of mixing coils on peak heights of 50 ppm aluminium at a flow rate of 5.0 mL min^{-1}.

In the flow system, the coil diameter is one of the main parameters which has affect on the dispersion. In this work, the coils of 0.5 and 1.0 mm diameter were used, and the result

is shown in Figure 3.14. It can be seen that the peak height from using the coil of 1.0 mm i.d. is higher and the reason for this result is that the sample and the reagent can mixed together better in the larger diameter coil. Nevertheless, the half peak width becomes broader when the coil diameter is increased. This can be concluded that the larger diameter of the coil is used, the more dispersion is obtained. From Figure 3.14, it is found that tailing from using the smaller coil is more than that from using the larger one since the sample in the previous coil has more friction with the tubing wall than in the latter one. In this aluminium analysis, the coil of 1.0 mm in diameter is reasonably selected owing to its higher sensitivity and sampling rate when comparing with the smaller coil.

3.2.2.4 Effect of the reagent concentration and temperature

The variation in concentration of reagent is shown in Figure 3.15. At higher concentration of alizarin red S, the calibration graph was linear in the higher range and the sensitivity was higher. The precipitation of alizarin red S was appeared at the concentration higher than 0.015 percent. However, when using the concentration of 0.015 % alizarin red S, it is difficult to adjust the reagent solution to zero with Spectronic 21 as detector. Therefore, the concentration of 0.010 % alizarin red s was used in this thesis to achieve the maximum sensitivity and the wide range of standard calibration graph.

In batch analysis, when the solution was heated to 60°C, the rate of reaction was faster than that at room

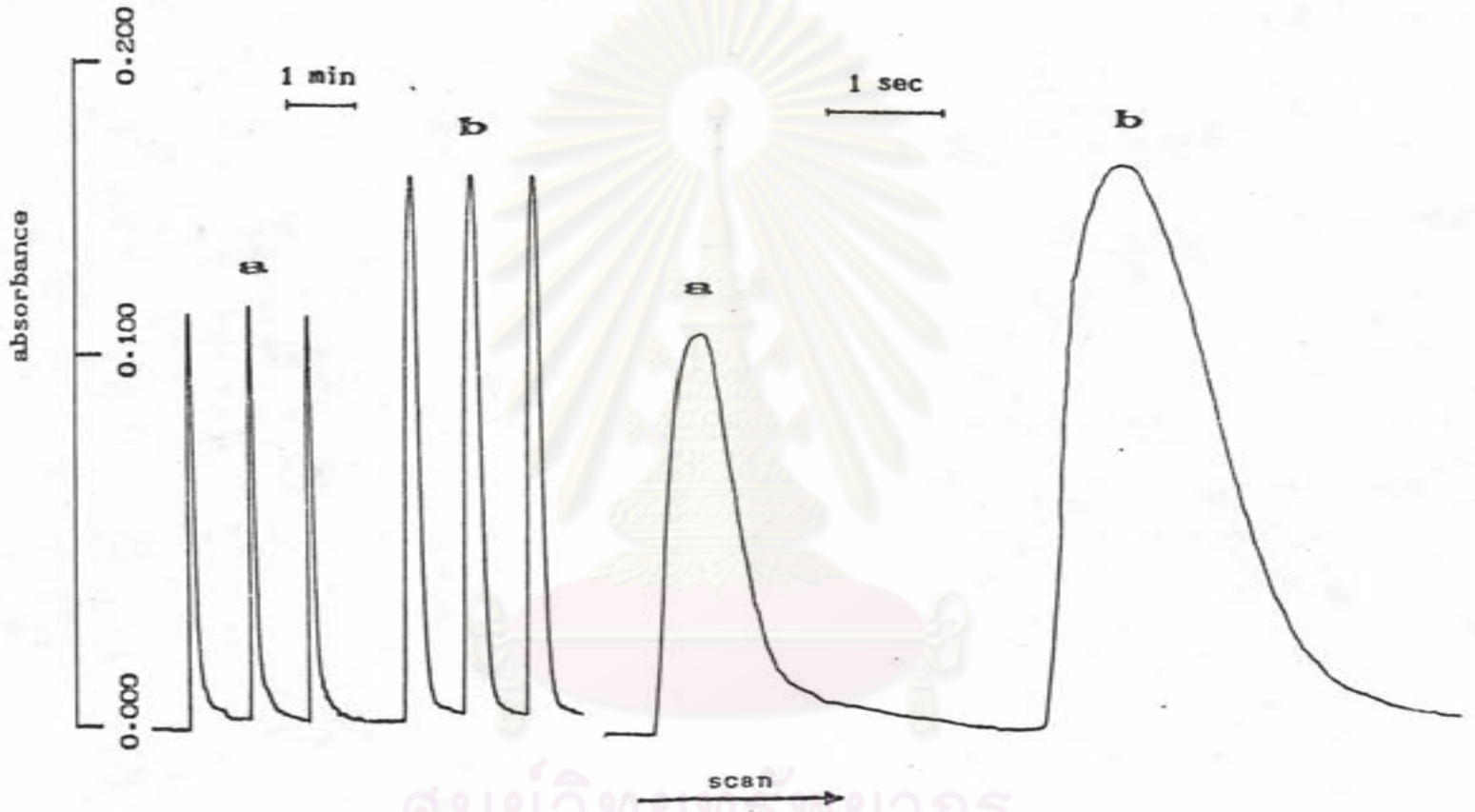

Figure 3.14 Effect of coils diameter on sample peaks at the flow rate of 5.0 mL min^{-1}: (a) 0.5 mm and (b) 1.0 mm, for 100 ul of 50 ppm aluminium solution.

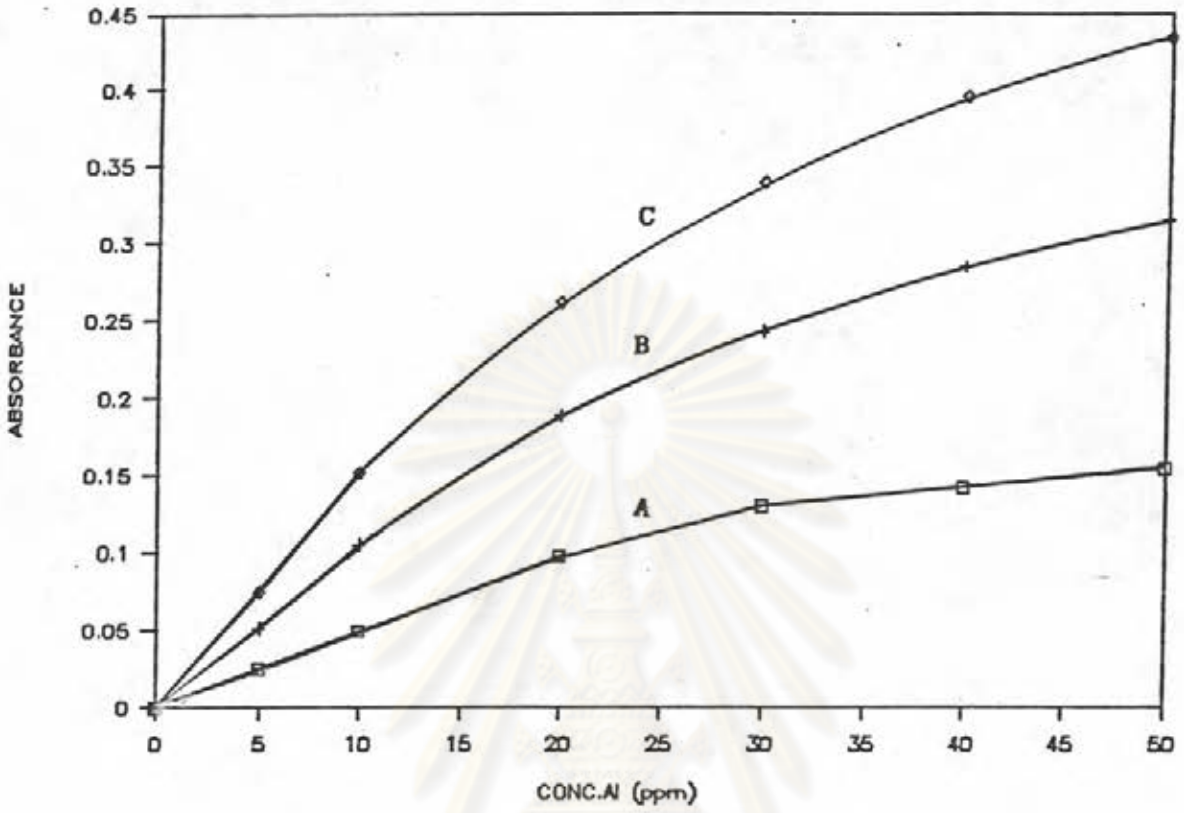

Figure 3.15 Effect of the reagent concentration in the flow injection system: A= 0.005 % alizarin red S; B= 0.010 % alizarin red S and C= 0.015 % alizarin red S.

temperature. In the flow injection system, the sensitivity was also higher when the reaction coil was heated to 60°C (by using water bath). However, the linear working range was narrower than that at room temperature. Heating the reaction coil would generate air bubbles that cause an error in flow injection analysis. The room temperature, therefore, was used in the determination of aluminium by flow injection analysis to achieve the wide range of standard calibration.

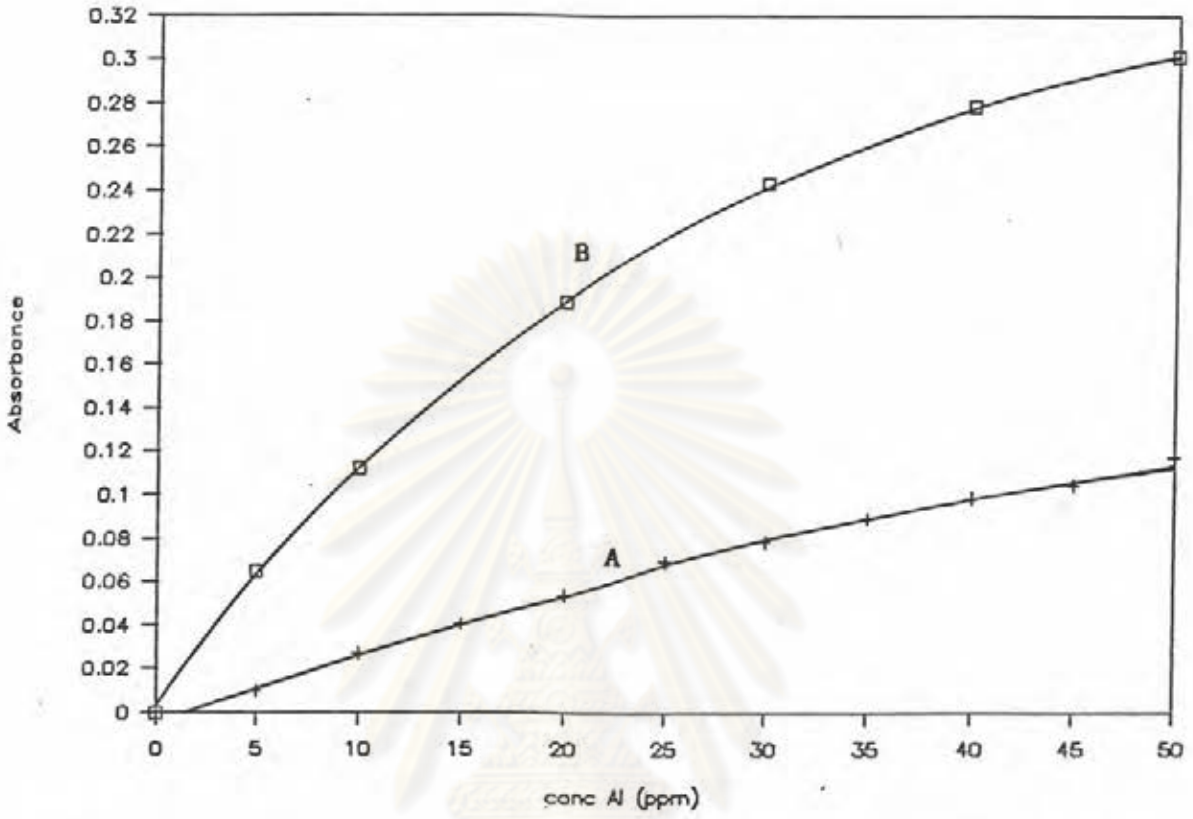

Figure 3.16 Effect of temperature on the linear range of standard aluminium solution: A= room temperature and B= 60°C

From the studies in section 3.2.1 and section 3.2.2, the suitable conditions for the aluminium analysis in the flow injection system can be deduced. The maximum absorption ratio of Al-alizarin red S complex and its reagent at 510 nm was used in the determination of aluminium. The pH of 0.01 % alizarin red S was 4.5 by using ammoniumacetate buffer solution. Addition of 200 mg/L of calcium ion to protect effect of calcium interference was required for the reagent solution. Effect of iron interference can be protected by using 0.04 % of thioglycolic acid as masking agent. Figure 3.17 shows different effectiveness of the masking agent as it

is present in the reagent solution and as it is in the standard solution. When thioglycolic acid was added to the reagent solution, some iron still react with alizarin red S to give higher absorbance while none of it would do when thioglycolic acid was added in the standard solution. Therefore, the 0.04 % thioglycolic acid should be added to sample solution to protect iron interference. From the optimization studies in flow injection system, the flow rate of 5.0 mL min^{-1} with 75 uL injection volume and the 150 cm tube length of 1.0 mm i.d. was used to achieve the maximum sensitivity and sampling rate in the determination of aluminium.

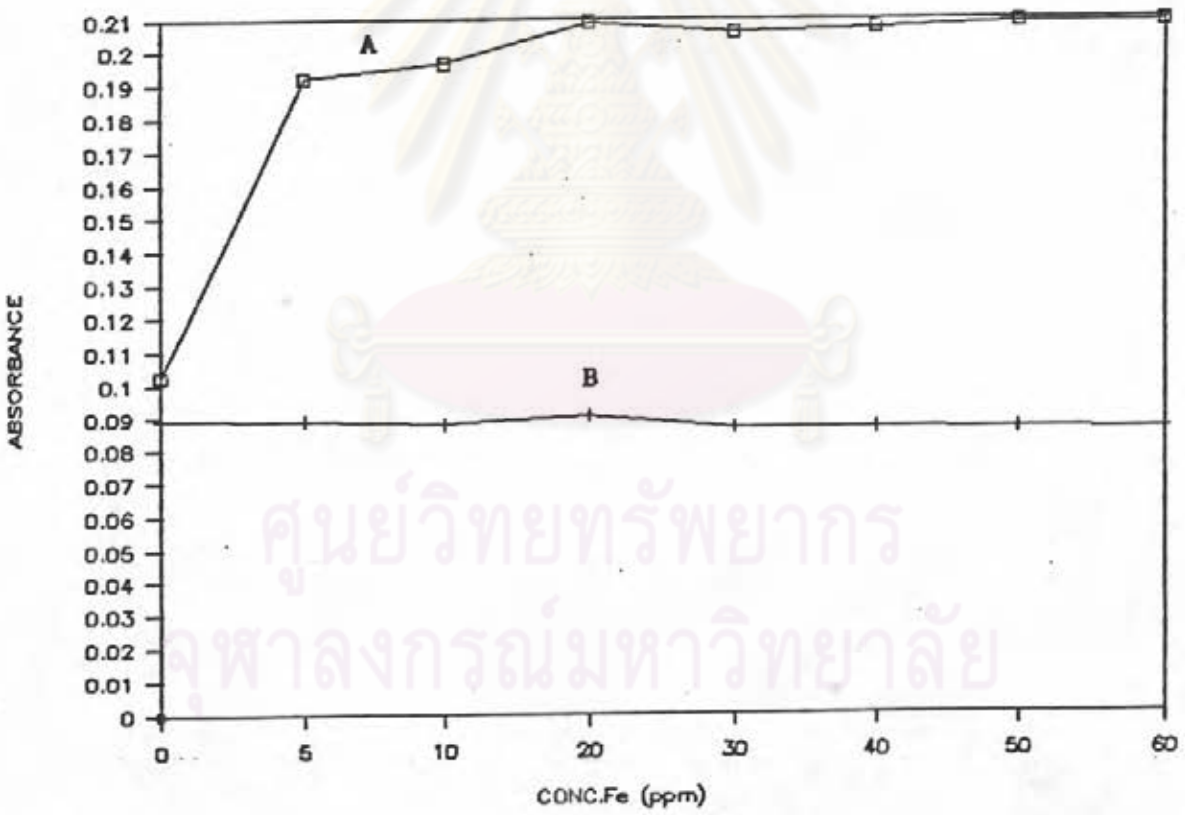

Figure 3.17 Effect of thioglycolic acid on the protection of iron by adding in the reagent solution (A) and in the standard solution (B).

3.2.2.5 Effect of Sampling Rate on Reproducibility and Carry-over

Sample interaction (carry-over) leading to inaccurate results, is a problem in flow injection system. Carry-over can be eliminated by employing a sufficient wash time between samples, allowing the dispersed tail approach to the base line closely. A long time between samples injection is usually required for the signal to reach the baseline. This effect of flush time therefore remained as a major factor limiting sampling rate in flow injection system. Figure 3.18 and Figure 3.19 demonstrate the effect of sampling rate on sample carry-over, precision and accuracy. The calculations of these values are summerized in Table 3.5. The peak height reproducibility depends on several experimental factors but the most important is the time between sample injections. The precision of this method is dependent on the reproducibility of the residence time of the sample in the system from the time of injecting

Table 3.5 Effect of sampling rate on reproducibility and carry-over

Sampling rate samples h^{-1}	Hmax Abs.	RSD	% Carry-over
60	0.1332	0.49	0
90	0.1317	0.66	0
120	0.1346	1.31	0
180	0.1335	1.41	0.75

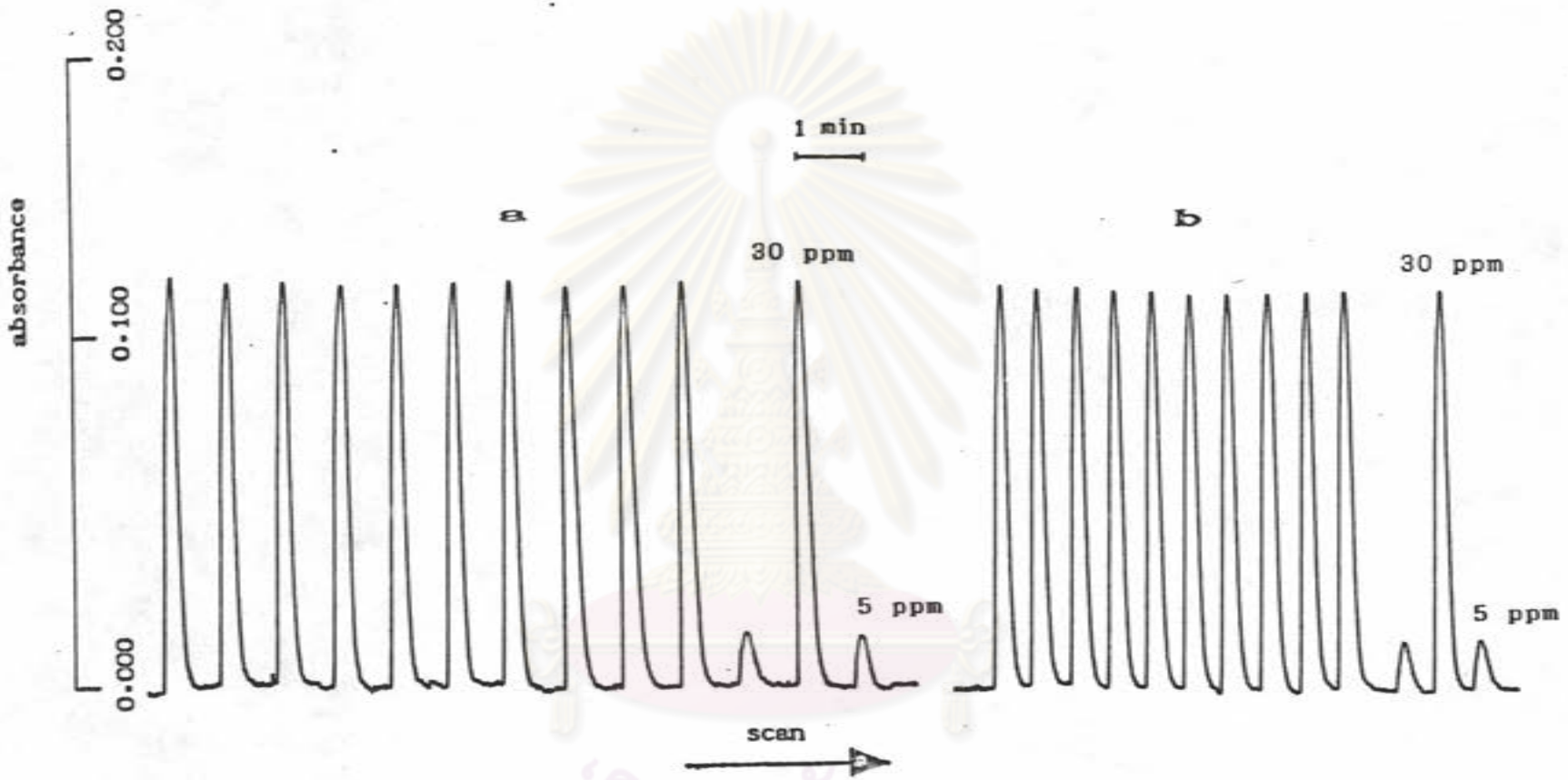

Figure 3.18 Carryover and precision of 10 replicate determinations of aluminium (concentration as shown) with (a)60 and (b)90 samples h^{-1}.

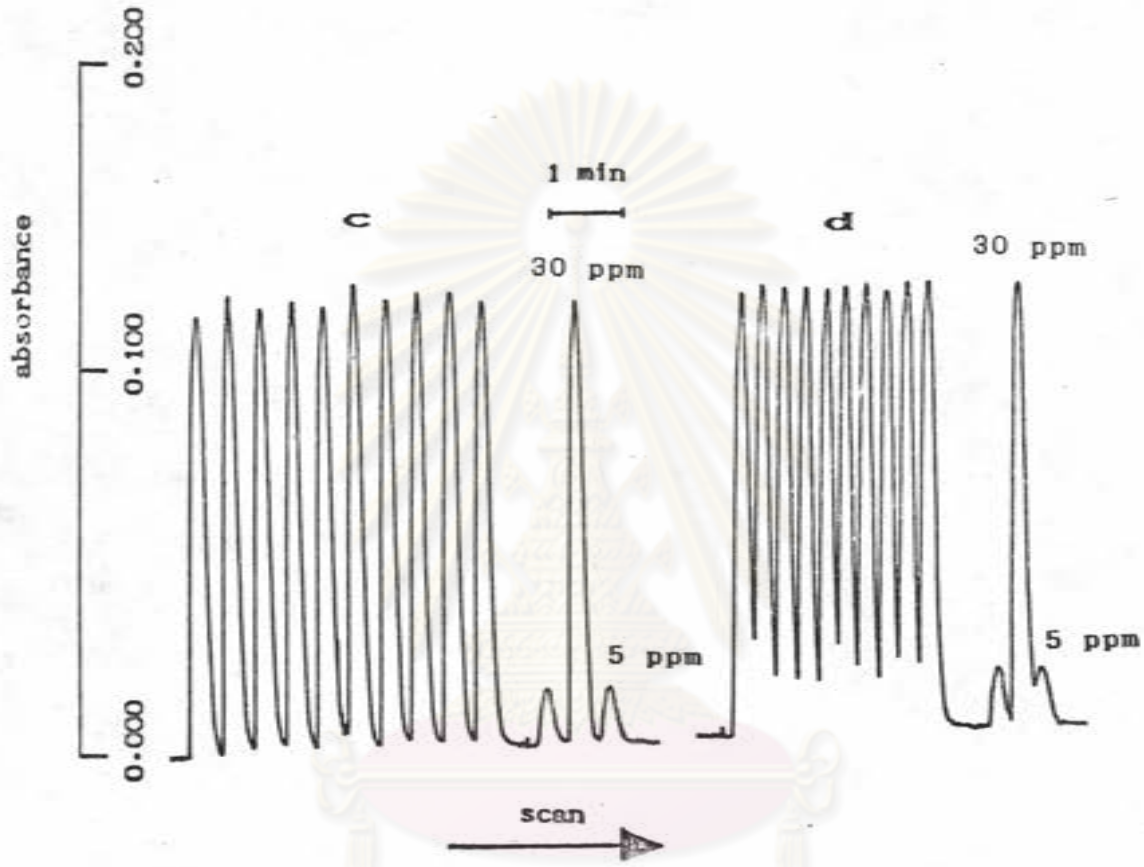

Figure 3.19 Carryover and precision of 10 replicate determinations of aluminium (concentration as shown) with (a)120 and (b) 180 samples h^{-1}.

to the peak maximum. The method precision therefore depends on maintaining a constant flow rate of reagent and the accurate timing of sampling and flush. In Table 3.5, the reproducibility and the carry-over are increased with the increase in sampling rate. There was no carry-over at sampling rate upto 120 samples h^{-1} and the reproducibility at 120 samples h^{-1} was 1.31 % .

3.2.2.6 Detection Limit and Linearity

Figure 3.20 shows the calibration plot for aluminium injected into 0.01 % alizarin red S in ammoniumacetate buffer solution (pH 4.5), using a concentration range 1.0 to 40.0 ppm of aluminium. It was found that there was a linear relationship between the concentration of aluminium and absorption in the range of 3.0-25.0 ppm with the correlation coefficient of 0.999. Detection limit for this determination was 2.0 ppm.

3.2.2.7 Interferences

In any analytical procedure, it is necessary to understand the interferences before any quantitative analysis is carried out. The possible sources of interferences in kaolin and lateritic clay such as calcium, magnesium, lithium, barium, potassium, zinc, cobalt, manganese(II), iron(III), silicate, nitrate, and phosphate were investigated. The interference study was carried out by using standard solution containing 20 ppm aluminium and the interference was considered to have effect if the detector response differed by more than 2 % relative from that of an interference-free standard. The effect of foreign ions on this determination is

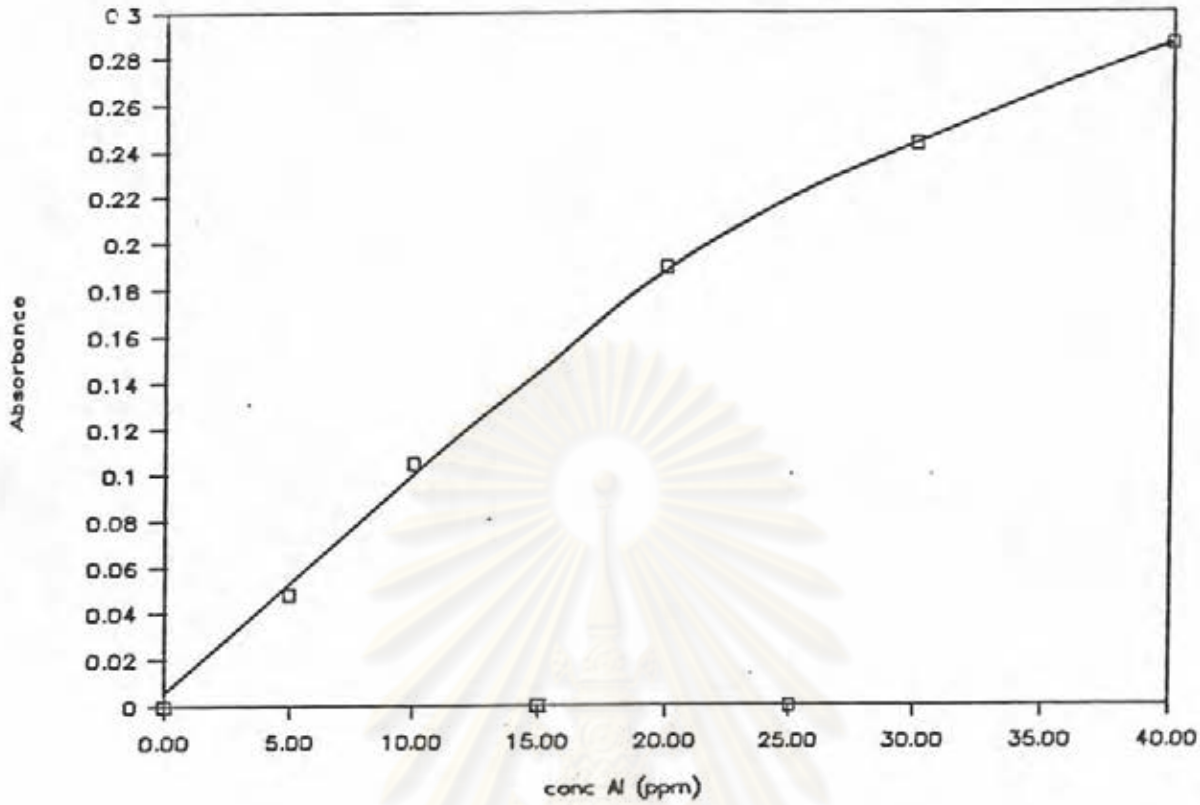

Figure 3.20 Calibration plot for aluminium

summerized in Table 3.6. By the above criterion, the ions that did not interfere when presented in concentrations up to 200 ppm were barium, calcium, copper, lithium, manganese, magnesium, potassium and nitrate. Zinc, phosphate and silicate in the concentration up to 100 ppm did not interfere. However, the quantity of these ions in the soil sample is very low and therefore has no effect in the aluminium determination. Interference from iron was masked by thioglycolic acid as described in section 3.2.1. Cobalt at the concentration greater than 50 ppm will increase the peak height of the detector response substantially. This effect of cobalt need not be concerned in this work as cobalt to aluminium concentration ratio is very low in kaolins and lateritic soils.

Table 3.6 Effect of cations and anions on the determination of 20 ppm aluminium.

Ions	Added as	Maximun added without interference, ppm
barium	$BaCl_2$	200
calcium	$CaCl_2$	200
cobalt	$Co(NO_3)_2$	50
copper	$Cu(SO_4)_2$	200
iron(III)	$FeCl_3$	50
lithium	LiCl	200
magnesium	$Mg(NO_3)_2$	200
manganese	$MnSO_4$	200
potassium	KCl	200
zinc	$ZnNO_3$	100
nitrate	KNO_3	200
phosphate	$(NH_4)HPO_4$	100
silicate	Na_2SiO_3	100

3.2.3 Determination of alumina in Kaolins and Lateritic soils

The total alumina in kaolins and lateritic soils were determined by the flow injection method. Furthermore, standard synthetic samples of kaolin and lateritic soil were also analysed to assess the accuracy of the method. The samples were digested

according to the procedure described in section 2.3.4. The results obtained by the proposed flow injection system comparing with the classical method for the synthetic samples are shown in Table 3.7. The results from both methods are in good agreement, however, the flow injection method shows better accuracy. From Table 3.7, percent recovery of alumina (45.0 %) in synthetic kaolin in the determination by the flow injection method and by the classical method are 100.02 and 99.78, respectively. For the determination of alumina (17.0 %) in lateritic soils, percent recovery was found to be 99.41 by the flow injection method and 101.2 by the classical method. However, the precisions of both methods are nearly equal. Table 3.8 describes the location of kaolin and lateritic soils samples in Thailand and the results of the determination of alumina in these samples are shown in Table 3.9. Figure 3.21 shows the determination of aluminium in some kaolins and lateritic soils in Thailand by flow injection analysis. The precision of the analysis of kaolins by both

Table 3.7 The determination of alumina in synthetic samples by flow injection analysis and by the classical method.

Samples	Flow Injection Analysis				Classical method			
	$\%Al_2O_3$ w/w	%Error	RSD	%Recovery w/w	$\%Al_2O_3$ w/w	%Error	RSD	%Recovery w/w
Synthetic kaolin (45.0 %)	45.1	0.22	1.29	100.02	44.9	0.22	1.88	99.78
Synthetic lateritic soil(17.0 %)	16.9	0.59	1.54	99.41	17.2	1.18	1.92	101.2

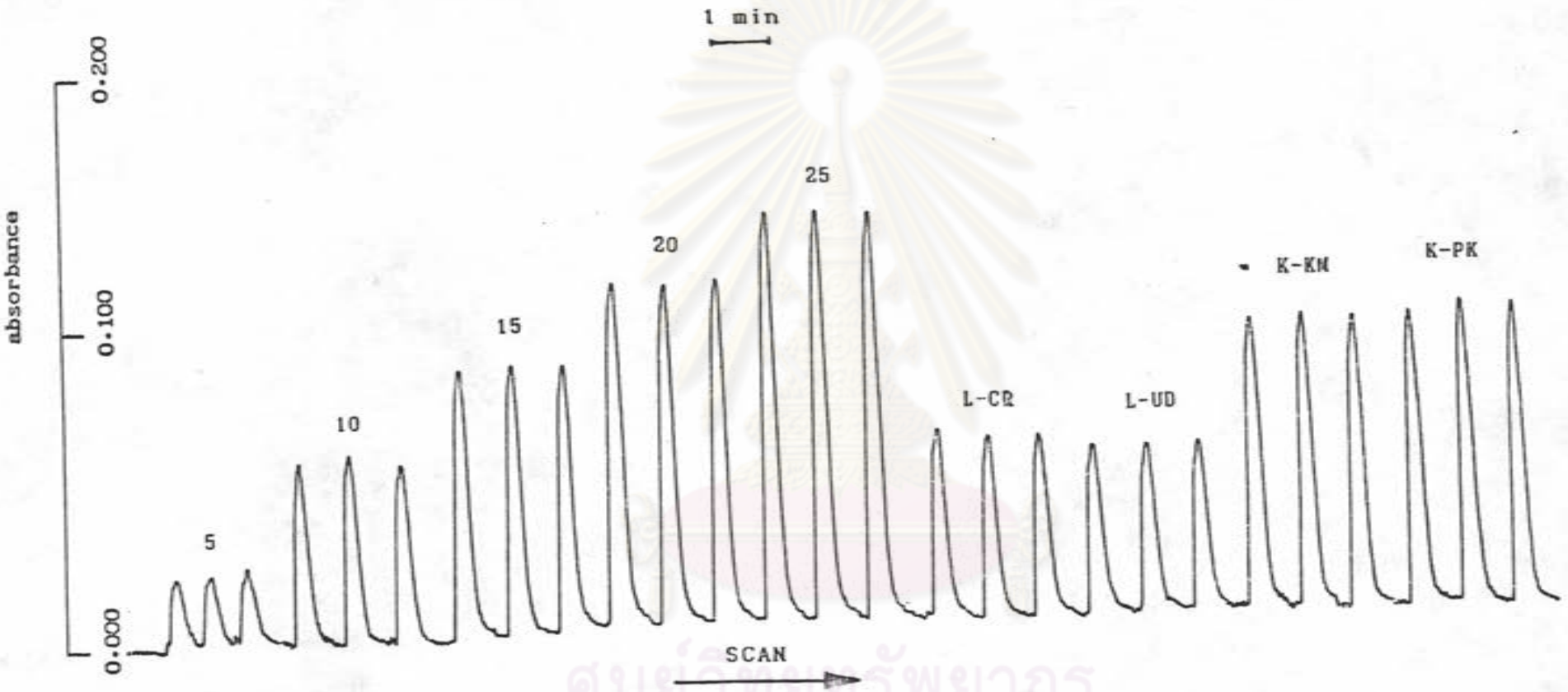

Figure 3.21 Determination of aluminium in some kaolins and lateritic soils by flow injection analysis

methods are similar. However, for the determination in lateritic soils, the percentage of alumina determined by flow injection method are slightly higher than that of the classical method. The lowest relative standard deviation is 1.36 % (sample code:L-KC) and the highest value is 2.19 % (sample code: L-CR) for the flow injection method while the lowest value of the classical method is 2.21 % (sample code: L-KC) and the highest is 3.96 % (sample code: L-UD).

Table 3.8 Description of sample code for location of the kaolins and the lateritic soils in Thailand.

Sample code	Location
K-VP	Wash kaolin from Vaieng Pa-Pao district, Chaieng-Rai province, Northern Thailand.
K-JD	Wash kaolin from Su-ngai Padi district, Narathiwat province, Southern Thailand.
K-PK	Wash kaolin from Tungkha district, Ranong province, southern Thailand.
K-KM	Wash kaolin from Khokmailai village, Prachinburi province, central Thailand.
L-CR	Chaieng-Rai province, Northern Thailand.
L-KC	Lateritic soil from Kanchanaburi province, Westhern Thailand.
L-NK	Lateritic soil from Nongkai province, North-Easthern Thailand.
L-UD	Lateritic soil from Udonthani province, North-Easthern Thailand.

Table 3.9 Determination of total alumina in the kaolins and the lateritic soils by flow injection method and the classical method.

Sample code	Flow Injection Analysis		Classical analysis	
	% Al_2O_3 (% W/W)	RSD	% AL_2O_3 (% W/W)	RSD
K-VP	41.45	1.00	41.60	1.86
K-JD	40.12	1.76	40.62	1.05
K-KM	39.44	1.43	39.50	1.20
K-PK	39.78	1.47	39.94	1.33
L-CR	22.64	2.19	22.99	2.28
L-KC	41.29	1.36	40.96	2.21
L-NK	13.54	1.68	13.66	3.93
L-UD	20.46	2.00	20.98	3.96

However, the analysis of alumina by the classical procedure was very difficult and used a long analysis time for each samples. In the determination of alumina by the classical method, the percentage of alumina was obtained by subtracting per cent of mixed oxide (% R_2O_3) with per cent of iron oxide and titanium oxide. The analysis of alumina by flow injection method was very rapid and gave an accurate and reproducible result. Sample throughput of 120 samples per hour was obtained with no carryover and was applicable to a wide range of alumina content.

3.3 Determination of Iron Oxide

3.3.1 Optimization studies on the Fe-thioglycolate complex in batch analysis.

Complex formation between iron and thioglycolate has been made of analytical use in the colorimetric determination of iron and in the separation of iron from the other metals. In air-saturated ammoniacal medium, a deep purple-red complex is formed regardless, wheather the iron was present initially in the ferrous or ferric state. Figure 3.22 shows the visible spectrum of 0.25 mg ferric ion in

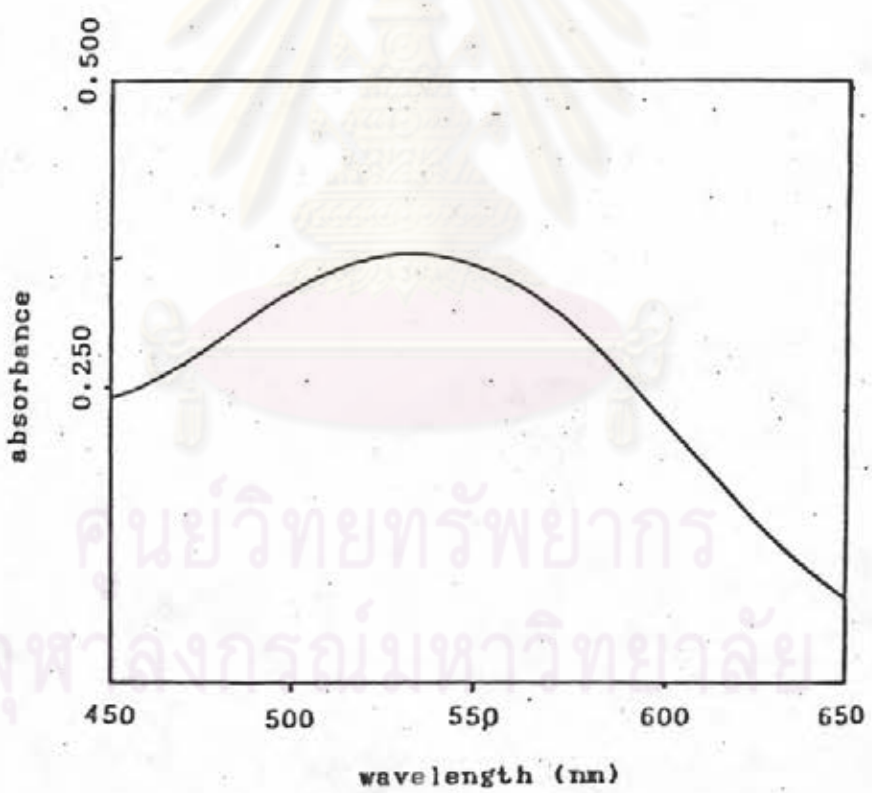

Figure 3.22 Visible spectrum of iron thioglycolate complex; 0.25 mg iron in 50 mL of 0.4 % thioglycolate in 0.3 M ammonia solution measured with the blank solution.

0.4 % of thioglycolate in 0.3 M ammonia solution measured against blank solution. The maximum absorbance was at 535 nm and this result agreed well with that of Leussing (42).

The rate of the formation of iron-thioglycolate at 25°C for iron concentration of 0.25 mg and 50 mL of 0.4 % thioglycolate in 0.3 M ammonia solution is shown in Figure 3.23. It took about one minute for the formation of iron-thioglycolate complex to reach 95 % complete reaction. This indicates that the formation of this complex is extremely rapid.

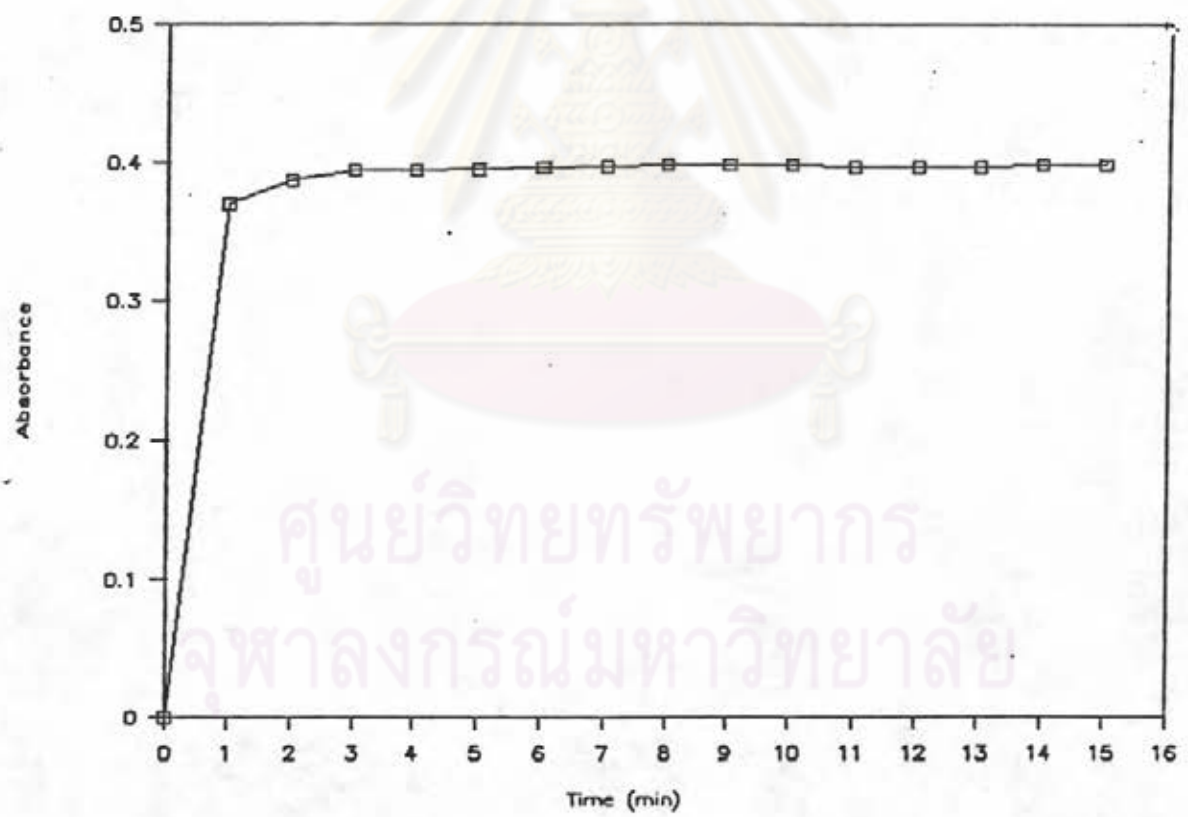

Figure 3.23 The rate of the formation of iron-thioglycolate complex; 0.25 mg iron in 50 mL of 0.4% thioglycolate in 0.3 M ammonia solution.

Effect of pH on the complex formation was studied by the use of various ammonium chloride buffer solution. Table 3.10 shows the effect of pH on the complex formation. From the results in Table 3.10, the pH from 8.0 to 10.5 have negligible effect on the complex formation. However, in the acid medium (pH 6.5-7.5) the color of complex was faded. Therefore, in the determination of iron by the use of thioglycolate method, the pH of reagent solution should be kept to basic not lower than 8.0 .

Table 3.10 Effect of pH on the formation of iron-thioglycolate.

pH of buffer solution	Fe added (mg/50 mL)	Absorbance	Fe found (mg/50 mL)
10.5	0.140	0.353	0.140
10.0	0.140	0.355	0.141
9.5	0.140	0.356	0.141
9.0	0.140	0.354	0.140
8.5	0.140	0.356	0.141
8.0	0.140	0.370	0.146
7.5	0.140	0.039	0.025
6.5	0.140	0.030	0.022

3.3.2 Optimization of experimental parameters in the Flow Injection Analysis

3.3.2.1 Effect of Sample Injection Volume

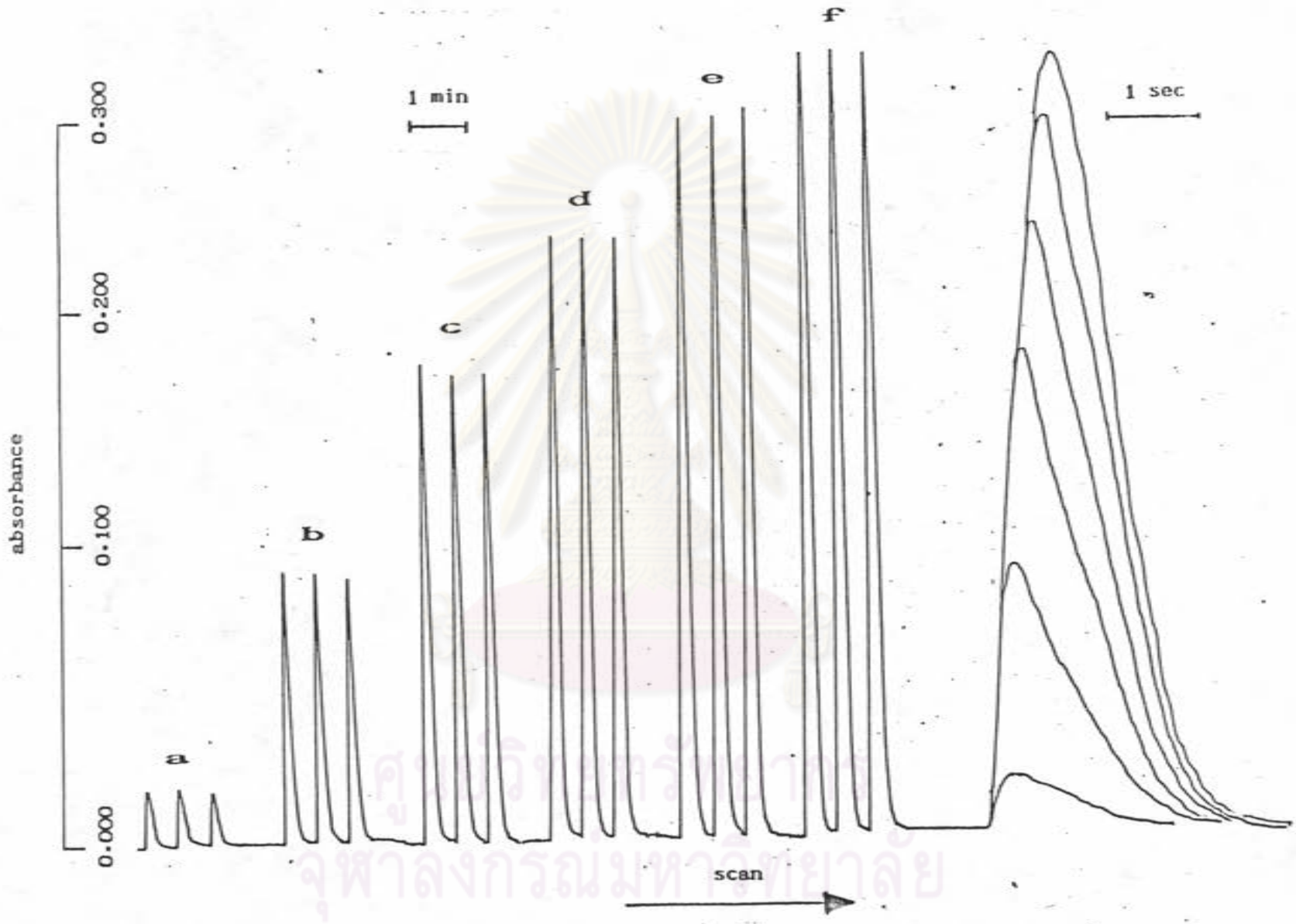

Figure 3.24 Effect of sample injection volume on sample peak for 15 ppm standard iron solution at the flow rate of 5 mL min^{-1} by using 100 cm i.d. coil length; (a) 10, (b) 50, (c) 100, (d) 150, (e) 200 and (f) 250 ul.

The absorption signals from injection of various sample volumes of 15 ppm standard iron solution are shown in Figure 3.24. The peak heigths after injection of each volume were plotted against the injection volume as shown in Figure 3.25. Increase in injection volume from 10 uL to 250 uL was found to increase peak height.

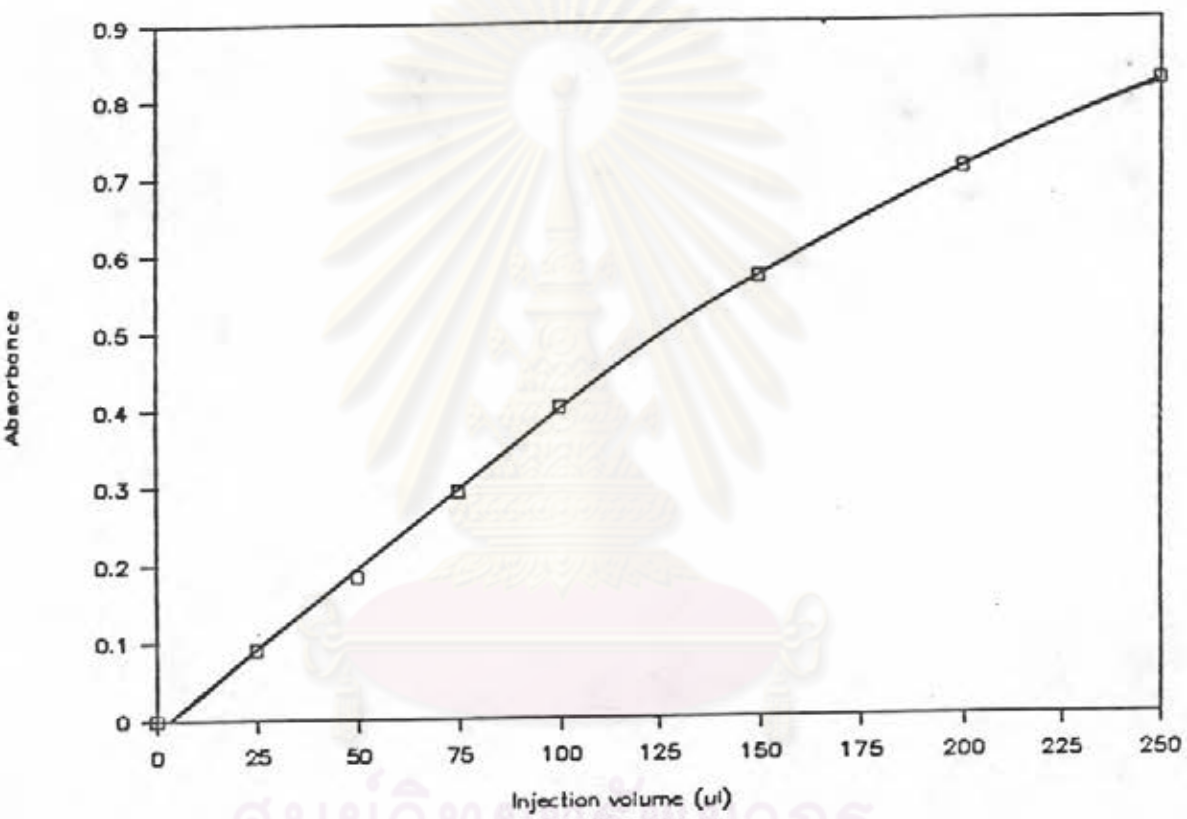

Figure 3.25 Effect of sample injection volume on peak height for 15 ppm of iron at the flow rate of 5.0 mL min^{-1}.

3.3.2.2 Effect of residence time

As it might be expected for the sample zone behavior in this system, the residence time of sample was found to

have a marked effect on the dispersion and the time required for the complex formation. The flow rate of carrier stream is one parameter that has effect on the residence time. For the studies on the effect of flow rate, sample peaks were recorded at various flow rates after injecting 100 uL of 15 ppm standard iron solution as shown in Figure 3.26. The results from Figure 3.26 are summerized in Table 3.11 showing the reproducibility, the widths for base line peaks, together with the calculated sampling rate. With the bore and pathlength fixed, increasing flow rate from 0.1 to 1.0 mL min^{-1} caused the slightly decrease in peak height. These results demonstrate that the rate of complex formation at this range of flow rate were more significant than the dispersion of sample zone. However, increasing the flow rate from 2.0 to 5.0 mL min^{-1}, the peak height was increased. It can be also concluded that at these flow rates, dispersion of sample zone was more significant than the rate of complex formation. Although, variation in flow rate gives various peak heights, they were not distinctively different. The base line peak width and hence calculated sampling rate for each flow rate are tabulated in Table 3.11. The peak width was found to be inversely proportional to the flow rate. The use of a high flow rate was shown to be advantageous by allowing higher sampling rate, because the rate of sampling is mainly dependent on the dispersion in the carrier stream.

The residence time of sample can be varied not only by the flow rate of the carrier stream but also by the size of transmission tubing. Coil of 1.0 mm i.d. with length in the range of 50-200 cm were used to demonstrate effect of coil length on sample peak, as shown in Figure 3.27. Increase in residence time by increasing coil length shows the decrease in peak height and the

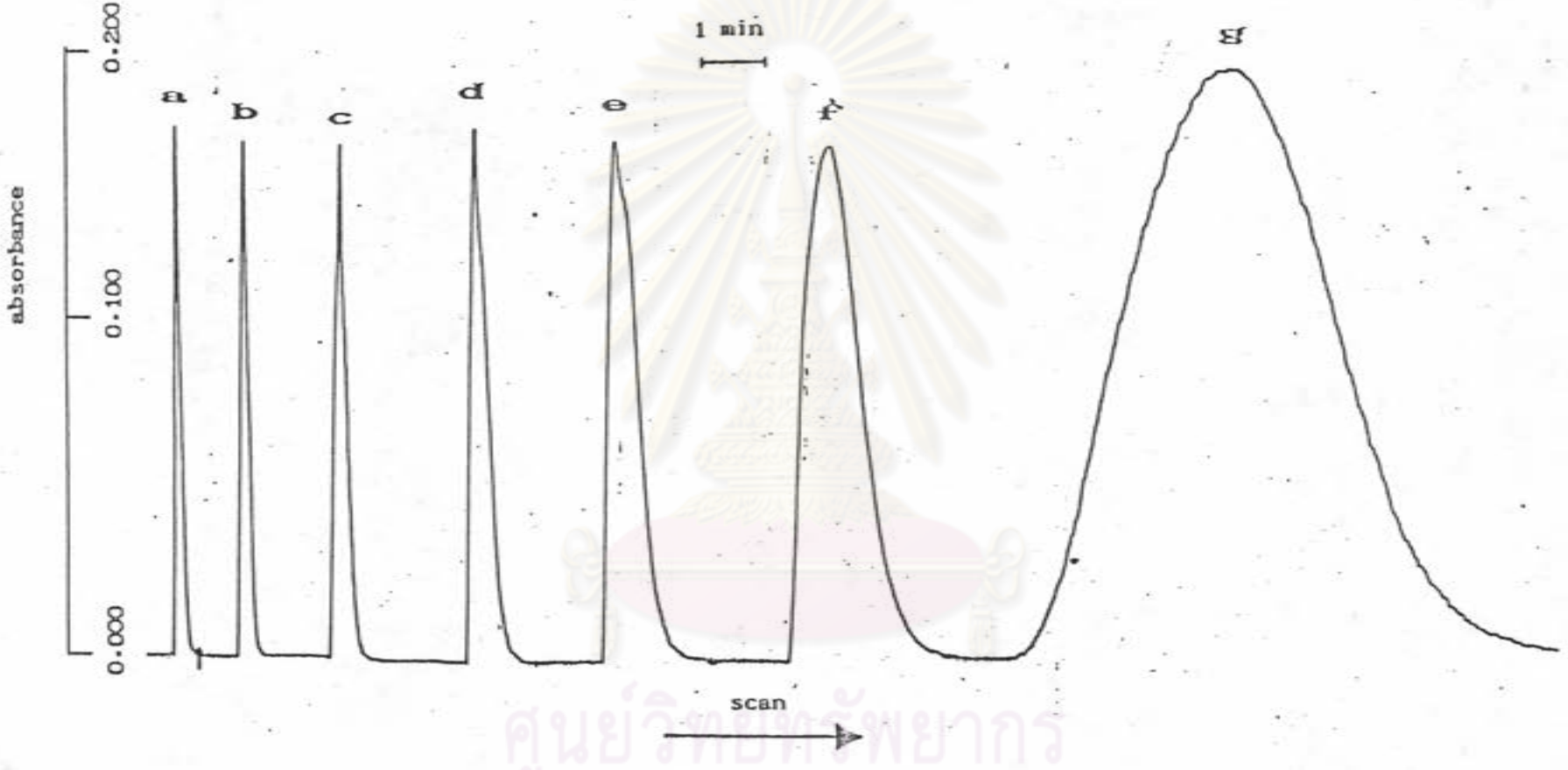

Figure 3.26 Effect of flow rate on response time of 100 ul of 15 ppm iron injected at various flow rate; A= 5.0 mL min^{-1}; B= 4.0 mL min^{-1}; C= 3.0 mL min^{-1}; D= 2.0 mL min^{-1}; E= 1.0 mL min^{-1}; F= 0.5 mL min^{-1} and G= 0.1 mL min^{-1}.

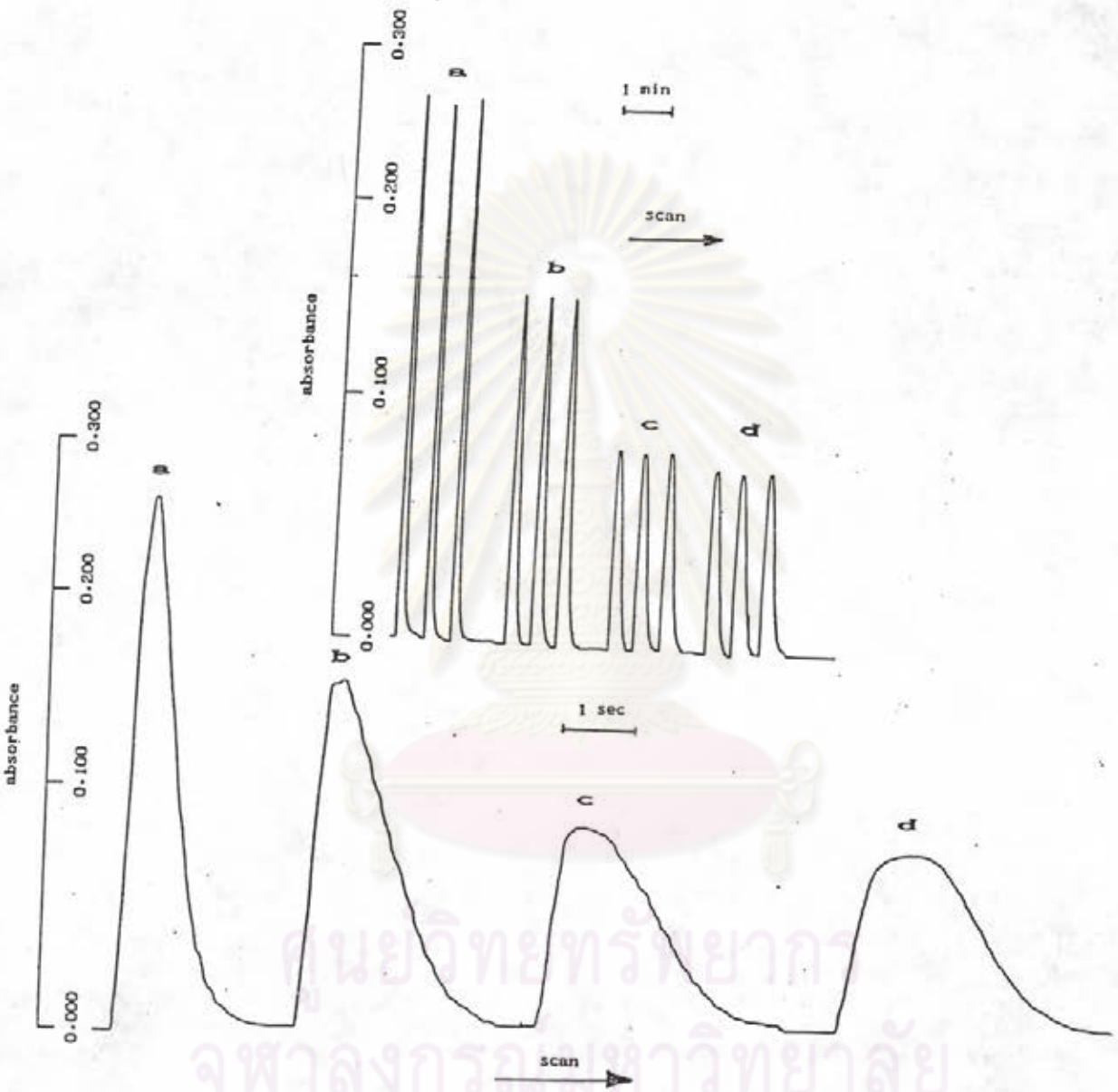

Figure 3.27 Effect of the length of 1.00 mm i.d. mixing coil on sample peak at the flow rate of 5.0 mL min^{-1}; (a) 50, (b) 100, (c) 150 and (d) 200 cm for injecting 100 uL of 15 ppm standard iron solution.

Table 3.11 Effect of flow rate on peak height, precision and sampling rates after manual injection of 100 uL of 15 ppm iron was injected at various flow rate by the use of 100 cm of 1.0 mm i.d. teflon tube.

Flow rate mL min^{-1}	Peak height Abs.	RSD	t_{base} sec	Sampling rate, h^{-1}
5.0	0.190	1.01	15	240
4.0	0.186	0.69	28	128
3.0	0.183	1.93	42	85
2.0	0.179	1.86	48	75
1.0	0.178	1.81	96	37
0.5	0.189	0.83	174	20
0.1	0.215	1.85	570	6

increase in peak tailing. The effect of coil length is very similar to the effect of dwell time in a flow injection system described by Ruzicka and Hansen (22). This indicated that the rate of complex formation between iron and thioglycolate was very fast therefore, the peak height was controlled by the dispersion in the flow system.

In the flow system, the coil diameter is one of the main parameters which has effect on the dispersion of the system. In this work, the coils of 0.5 and 1.0 mm i.d. were used, and the result was shown in Figure 3.28. The result of this effect was adversely to that of aluminium. The peak height from using 0.5 mm i.d.

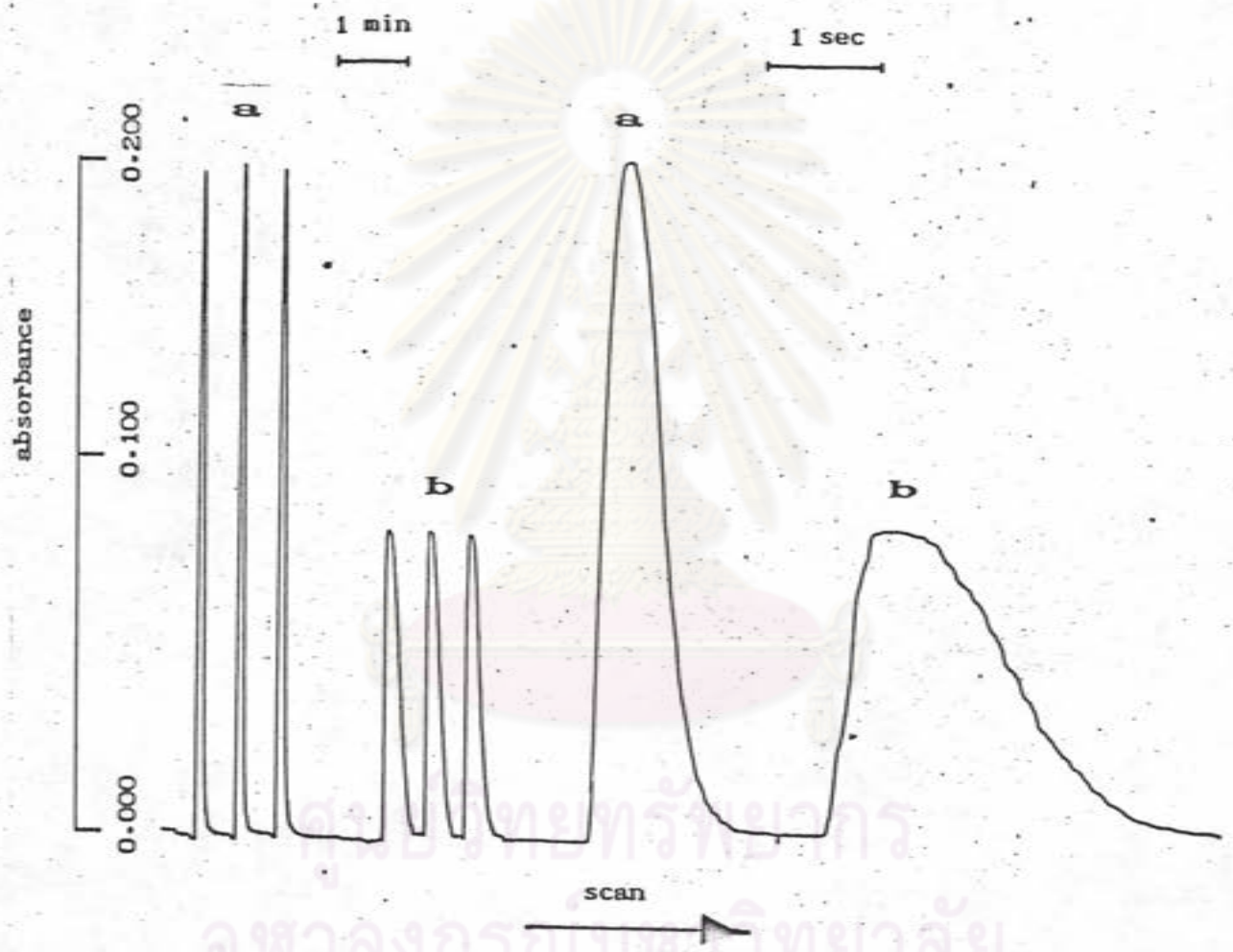

Figure 3.28 Effect of diameter coils of 150 cm coil length on sample peak at the flow rate of 5.0 mL min^{-1}; (a) 0.5 and (b) 1.0 mm for 100 uL 15 ppm of standard iron solution.

was heigher than that of 1.0 mm i.d. This result is similar to the effect of coil diameter in a flow injection system described by Ruzicka and Hansen (22) for the simplest flow system which has no chemical reaction occured. For the flow system that is controlled only by dispersion, the increasing of coil diameter gives the decrease in peak height and the increase in peak tailing of recorded signal, caused by the increase in dispersion.

From the study in section 3.3.1 and section 3.2.2, it can be concluded that for the determination of iron in the flow injection system, the wavelength must be fixed at 535 nm. The optimum manifold of 50 cm with 1.0 mm i.d. tubing was employed with the flow rate of 5.0 mL min^{-1}. The study also shows that the peak height is directly proportional to the sample injection volume. However, the sample frequency is inversely proportional to the sample injection volume. Therefore, in this work the same sample injection volume as that was used in the determination of aluminium, 75 uL, was selected.

3.3.3 Flow Injection Analysis of Iron

The determination of iron by using thioglycolate as reagent must be carried in the basic medium (ammoniacal medium). This leads to the problem in the analysis of kaolins and lateritic soils as the precipitation of metal hydroxides such as aluminium hydroxide, titanium hydroxide, etc., would occured. Figure 3.29 shows the effect of the precipitation of metal hydroxide on the peak in flow injection system. This effect gives an unreproducible peak height and the appearance of the peak tailing.These are because the distribution of

precipitate is unreproducible in flow-through cell. These precipitate was also difficult to flush out from the cell. It was found that the concentration of 8 % ammonium citrate can protect the precipitate of metal hydroxides. However, in the presence of ammonium citrate, the sensitivity of the determination of iron was lower than that without ammonium citrate.

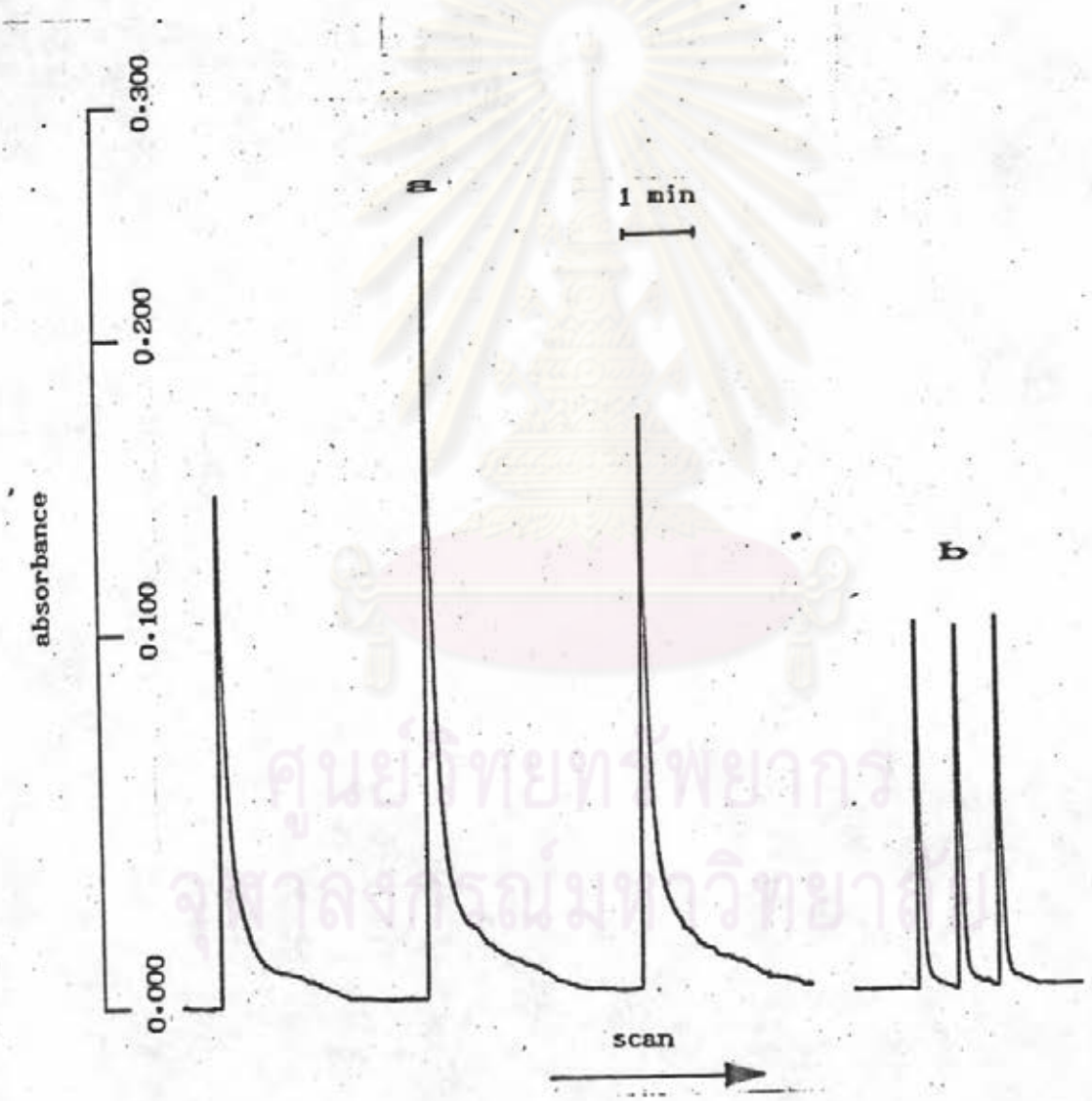

Figure 3.29 Effect of precipitation of metal hydroxide in basic medium (a) and protect by using 8 % ammonium citrate (b).

The variation in concentration of thioglycolate is shown in Figure 3.30. When using the concentration higher than 0.4 % thioglycolate, the deviation from linearity in calibration curve was obtained. The concentration of 0.4 % thioglycolate was found to be the most appropriate as it gives the linear calibration with the correlation factor of 0.999 in the range of 1.0-40.0 ppm iron.

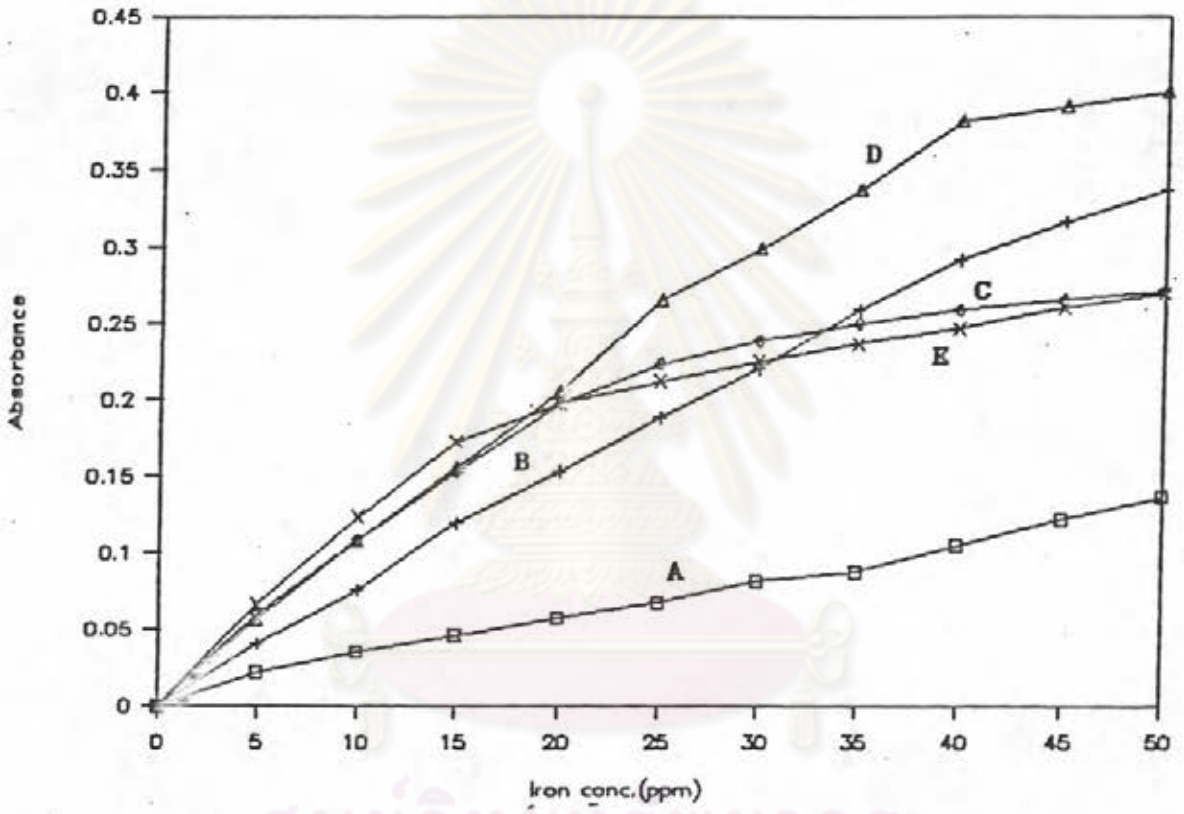

Figure 3.30 Effect of reagent concentration in flow injection system: A= 0.1 %, B= 0.2 %, C= 0.3 %, D= 0.4 %, and F= 0.5 % thioglycolic acid.

3.3.3.1 Precision and Carry-over

Peak height recording of 10 replicates at various sampling rates are shown in Figure 3.31 and Figure 3.32

Calculation of sampling rate together with relative standard deviation(RSD), carry-over (% CO) and reagent consumption are summerized in Table 3.12. It was clear from Table 3.12 that the peak height reproducibility depended on the sampling rate. A high sampling rate allows very short interval between sample injections and therefore causes large error in injection volume when using the manual injection. Standard solution in the concentration of 1.0 ppm and 30.0 ppm of iron were used for the determination of carry-over. In order to obtain negligible carry-over, sufficient time for injection must be allowed for the dispersed tail to approach the base line. Table 3.12 shows that the sampling rate upto 180 samples h^{-1} can be obtained with very low carry-over.

Table 3.12 Precision, Carry-over and Reagent consumption at varicus sampling rates obtained by injecting 30.0 ppm and 1.0 ppm of iron at the flow rate of 5.0 mL min^{-1}.

Sampling rate s h^{-1}	RSD	% CO	Reagent consumption, mL
60	1.26	0.00	5.0
90	1.70	0.00	3.3
120	2.05	0.00	2.5
180	2.40	0.40	1.7

3.3.3.2 Detection limit and Linearity

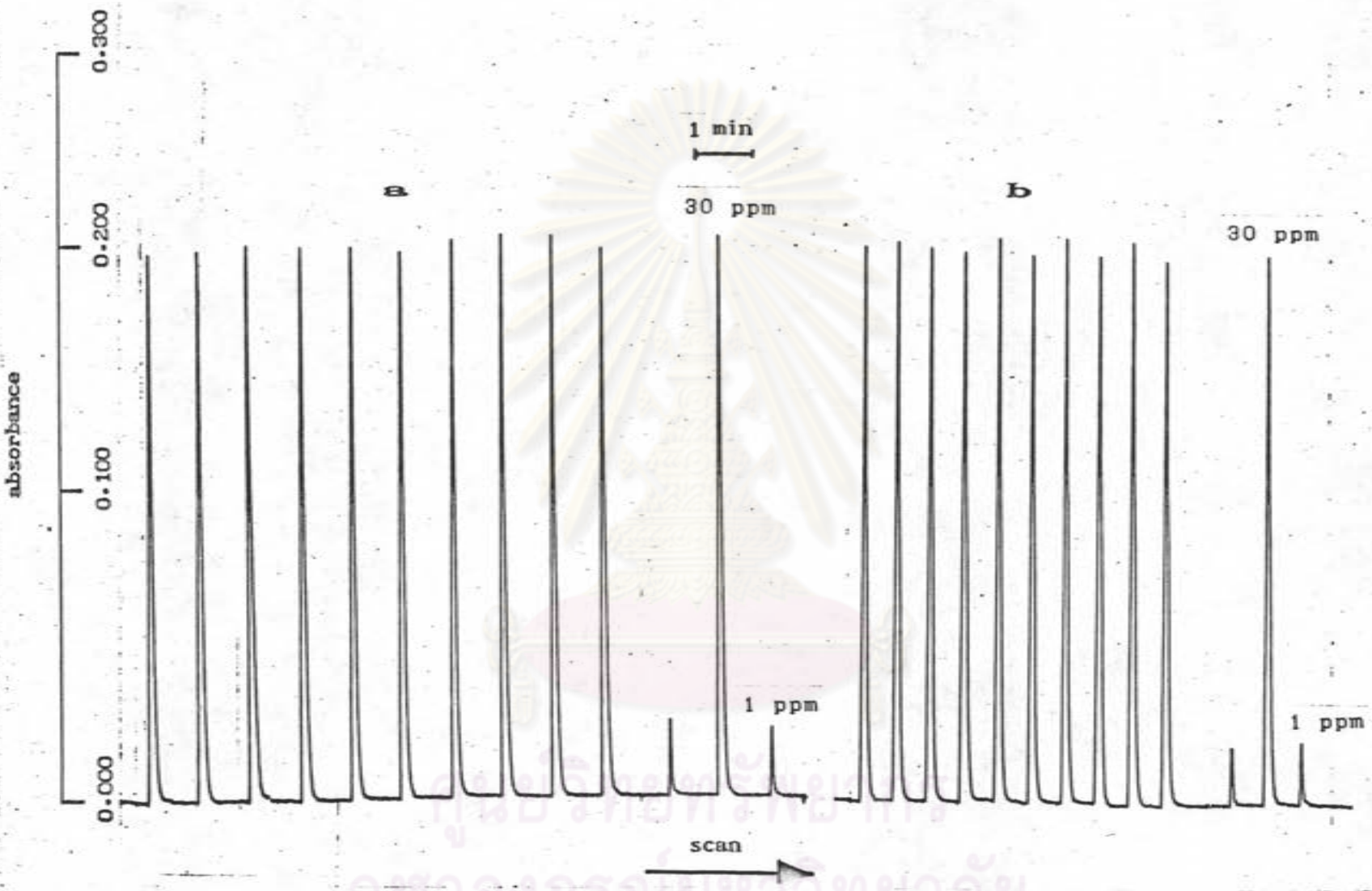

Figure 3.31 Carryover and precision of 10 replicate determinations of iron (concentrations as shown) with (a) 60 and (b) 90 samples h^{-1}.

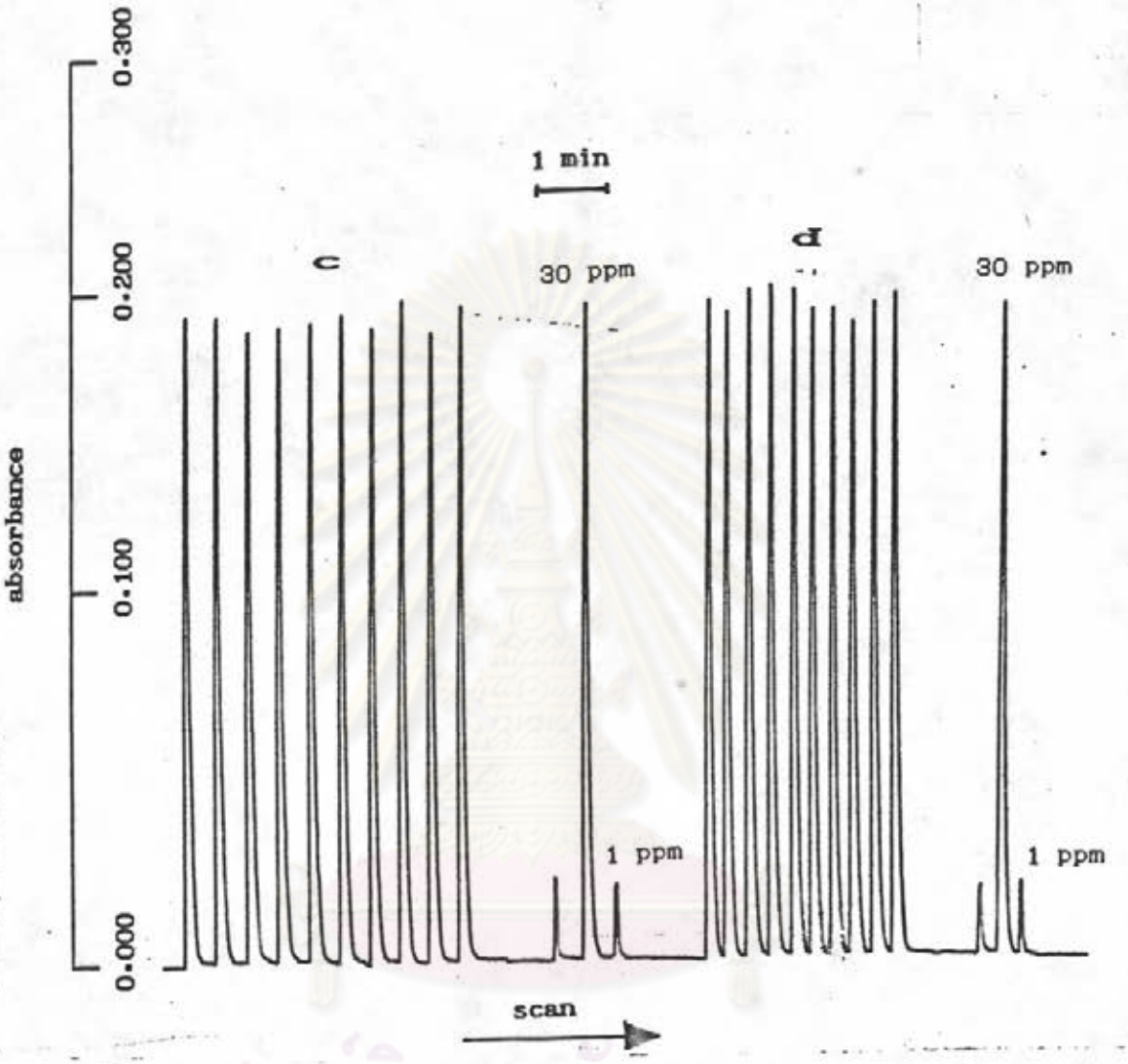

Figure 3.32 Carryover and precision of 10 replicate determinations of iron (concentration as shown) with (c) 120 and (d) 180 samples h^{-1}.

Figure 3.33 shows the calibration plot for iron injected into 0.4 % ammonium-thioglycolate , using a concentration range 0.0 to 50.0 ppm of aluminium. It was found that there was a linear relationship between the concentration of iron and absorption in the range of 1.0 to 40.0 ppm with the correlation coefficient of 0.999. Detection limit for this determination was 0.25 ppm.

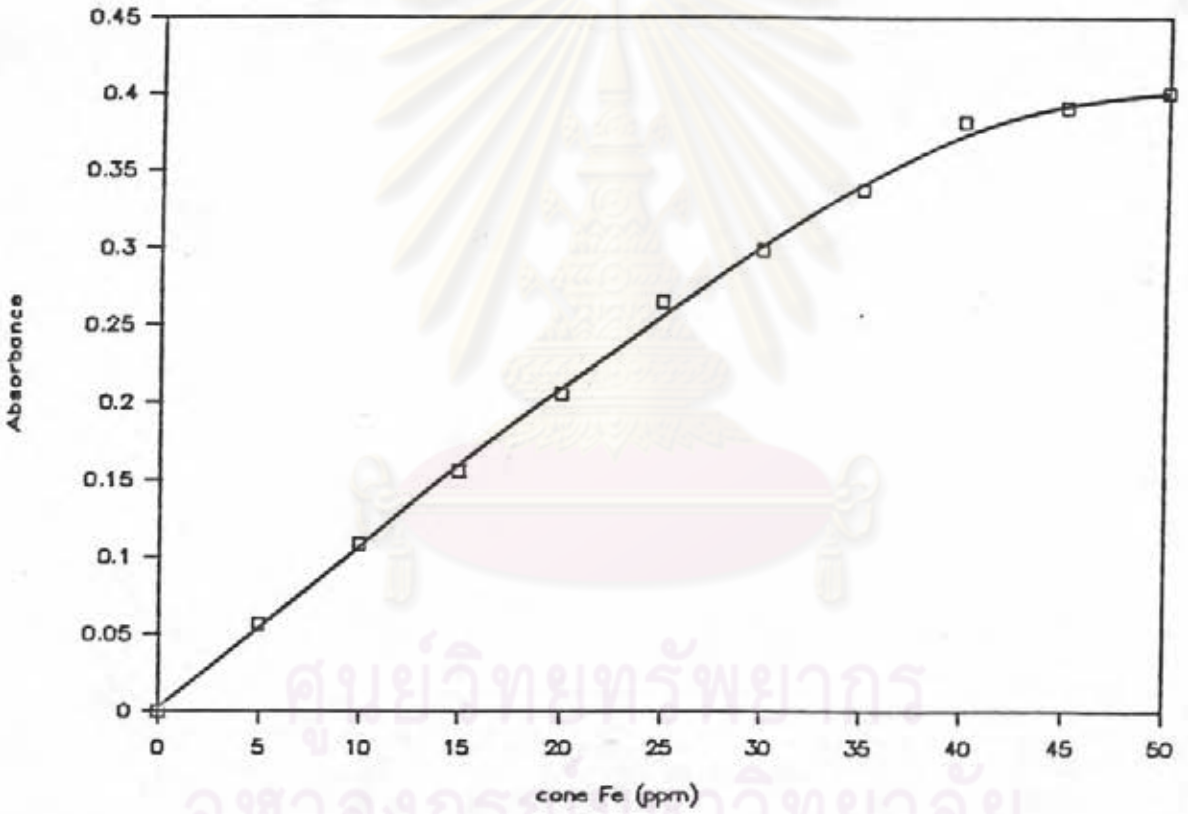

Figure 3.33 Calibration plot for iron

3.3.3.4 Interference

The similar interference study as in section 3.2.2.6 was carried out using standard solution containing 15 ppm of

iron. The effect of ions on this determination is summerized in Table 3.13 which shows that aluminium, barium, calcium, copper, lithium, manganese, magnesium, potassium, zinc, nitrate, phosphate and silicate do not interfere even though the concentration of these elements in the sample solution are as high as 200 ppm. Cobalt increased the peak height of iron by factor of 0.002 absorbance unit per 5 ppm of cobalt, therefore, 10 ppm cobalt will increased the peak height of 15 ppm iron by 2 % relative. However, the percentage of cobalt in soil especially kaolin is very small comparing with the percentage of iron. Consequently, a masking agent for cobalt is not nescessary.

3.3.4 Determination of iron oxide in kaolins and lateritic soils.

Table 3.14 shows the results for the determination of iron oxide in the synthetic kaolins and the synthetic lateritic soils by the flow injection method and by the classical method. The flow injection method was found to give better accuracy than the classical method. The results of iron oxide determination in various kaolins and lateritic soils in Thailand are shown in Table 3.15. By 10 replicates determination of each sample by the flow injection method, the relative standard deviation for kaolins did not exceed 4 % however, the one for lateritic soils was about 1%. The relative standard deviation for the kaolins by the classical method had the lowest and the highest values at 2.49 % and 10.13 %, respectively. In the flow injection analysis of the synthetic kaolin and the synthetic lateritic soil, percent recovery is 96.67 % and 99.45 %, respectively. However, the recovery of iron oxide by the classical method was found to be higher than 100 %, 109.33 % for synthetic kaolin and

Table 3.13 Effect of cations and anions on the determination of 15 ppm iron.

ions	Added as	maximun added without interference, ppm
aluminium	$AlCl_3$	200
barium	$BaCl_2$	200
calcium	$CaCl_2$	200
cobalt	$Co(NO_3)_2$	10
copper	$Cu(SO_4)_2$	200
lithium	LiCl	200
magnesium	$Mg(NO_3)_2$	200
manganese	$MnSO_4$	200
potassium	KCl	200
zinc	$Zn(NO_3)_2$	200
nitrate	KNO_3	200
phosphate	$(NH_4)HPO_4$	200
silicate	Na_2SiO_3	200

100.62 % for synthetic lateritic soil. For lateritic soils, the relative standard deviation of both methods are not greater than 2 %. However, the percentage of iron oxide determined by the flow injection method in kaolins was found to be lower than that of the classical method while in lateritic soils, both methods are in good agreement.

Table 3.14 The determination of iron oxide in the synthetic samples by flow injection analysis and by classical method.

Samples	Flow Injection Analysis				Classical method			
	$\%Fe_2O_3$ w/w	%Error	RSD	%Recovery w/w	$\% Fe_2O_3$ w/w	%Error	RSD	%Recovery w/w
Synthetic kaolin (1.50 %)	1.45	3.33	4.03	96.67	1.64	9.33	7.99	109.33
Synthetic lateritic soil(40.0 %)	39.78	0.55	1.02	99.45	40.25	0.62	0.89	100.62

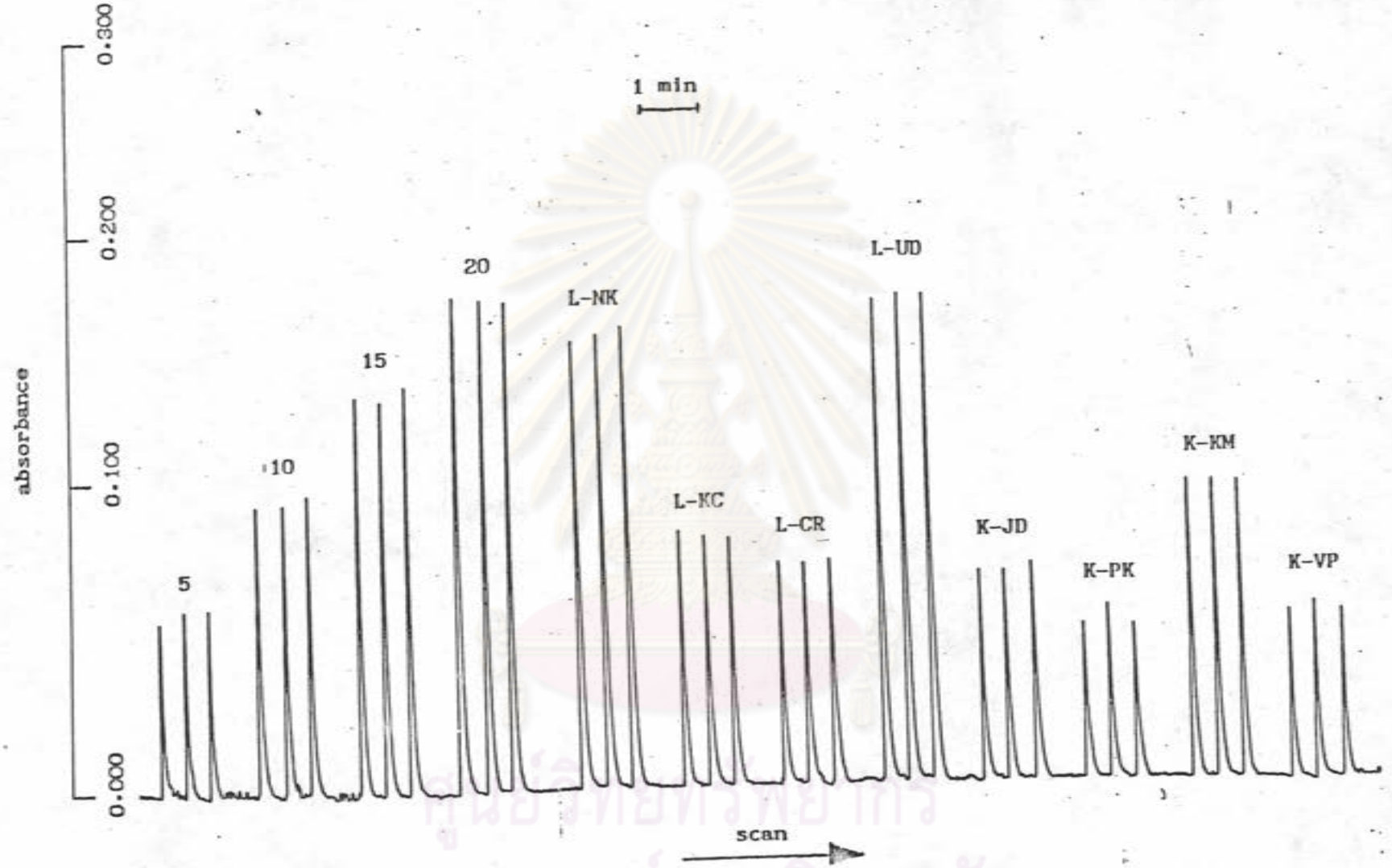

Figure 3.34 Determination of iron in some kaolins and lateritic soils by flow injection analysis

Table 3.15 Determination of total iron oxide in Kaolins and Lateritic soils.

Sample code	Flow Injection Analysis		Classical analysis	
	% Fe_2O_3 (% W/W)	RSD	% Fe_2O_3 (% W/W)	RSD
K-VP	1.12	3.66	1.20	10.13
K-JD	1.01	3.52	1.39	5.42
K-KM	1.61	3.10	1.67	2.49
K-PK	0.83	3.58	1.00	5.70
L-CR	16.66	1.27	17.18	1.54
L-KC	18.50	0.50	16.55	0.60
L-NK	38.49	1.70	38.77	1.44
L-UD	42.76	1.02	43.71	0.55

3.4 Determination of Silicon

3.4.1 Optimization studies in the Silicomolybdate complex in batch analysis.

The analytical methods for the determination of silica have been based upon the formation of silicomolybdate complex. Silicon will react with molybdic acid to form a yellow silicomolybdate complex. Solution of silicomolybdate was obtained by adding 3.0 mg of silicon into 50 ml of 0.06 M ammonium molybdate in 1 % sulfuric acid.

Figure 3.35 shows the ultraviolet spectrum of silicomolybdate measured against water and the blank solution and of molybdic acid measured against water. The maximum absorbance of silicomolybdate measured against the blank solution was at 355 nm. The absorbance of molybdic acid at 355 nm was high and by the use of single beam spectrometer (Spectronic 21) as the detector in this thesis, the absorbance of the blank solution can not be adjusted to zero. Therefore, the wavelength of 400 nm was employed in order to adjust the blank solution to zero in the determination of silicomolybdate.

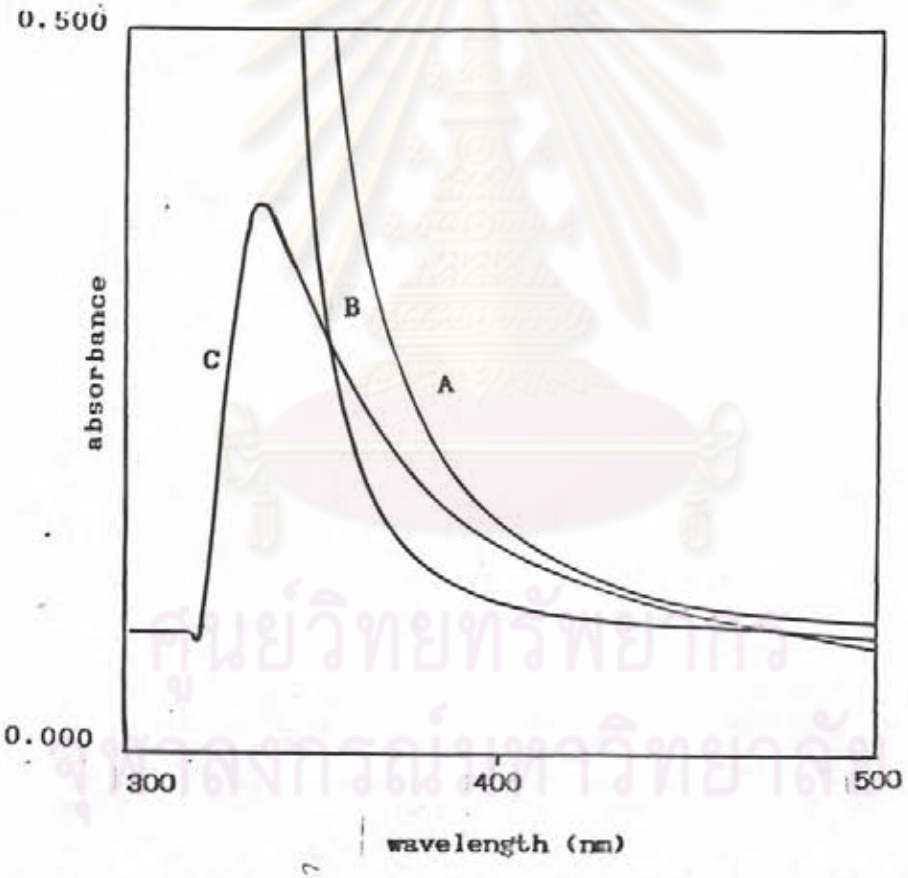

Figure 3.35 Ultraviolet spectrum of silicomolybdic acid : A= 0.03 M ammonium molybdate in 0.5 % sulfuric acid measured against water; B and C = 3.0 mg of silicon in 0.03 M ammonium molybdate in 0.5 % sulfuric acid measured against water and the blank solution respectively.

The rate of formation of silicomolybdate at 25 °C for silicic acid of 0.5 mg and 50 ml of 15.0 mg/ml ammonium molybdate in 1 % sulfuric acid was shown in Figure 3.36. The formation of silicomolybdate took about 5 min for 95 % complete reaction when the reagent was stored in a plastic bottle for 1 day and took about 8 min for the freshly prepared reagent. However, the reaction time was reduced to 3 min if the solution was heated to 50 °C and the fading of color would occur right after the complex formation was completed.

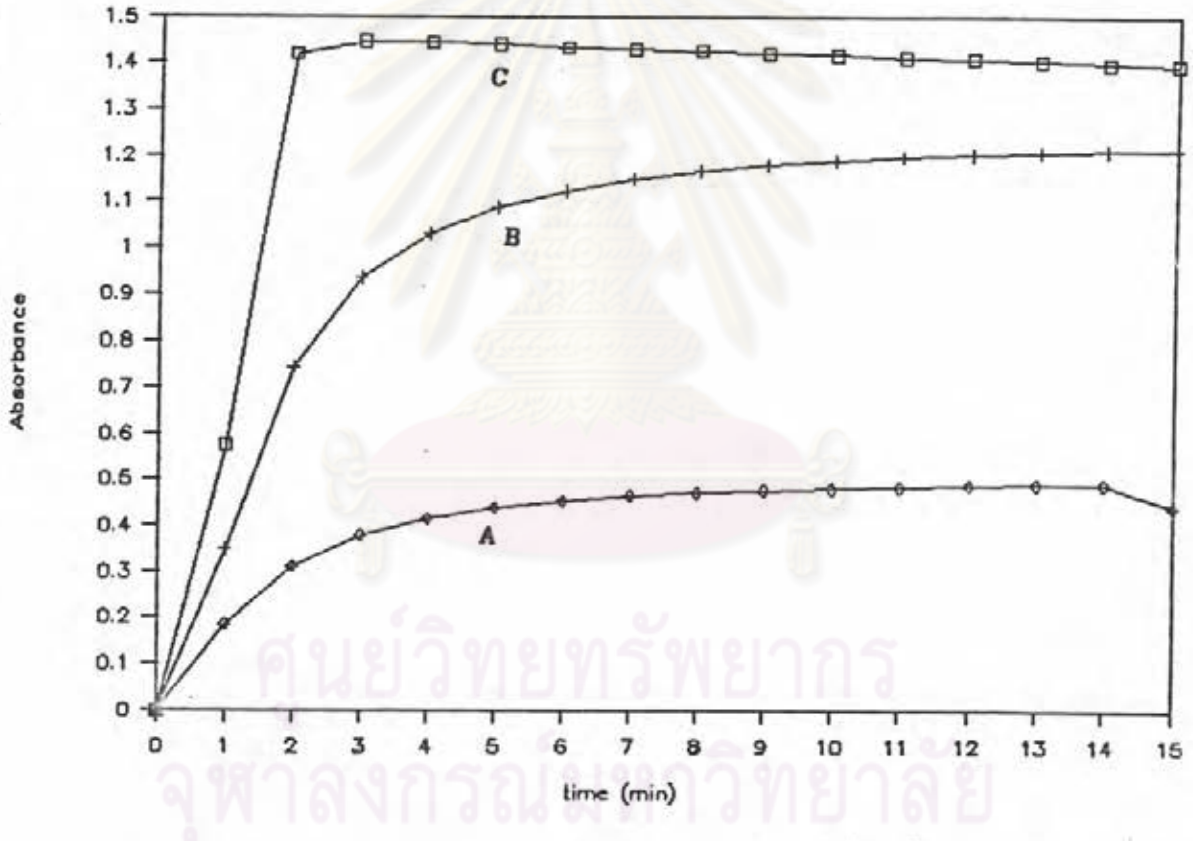

Figure 3.36 The rate of the formation of silicomolybdate complex with 0.5 mg silicic acid in 50 ml of 0.06M ammonium molybdate in 1 % sulfuric acid: A= freshly prepared reagent; B= reagent prepared after 1 day; C= freshly prepared solution was heated to 50 °C.

3.4.2 Optimization of experimental parameters in the flow injection analysis.

3.4.2.1 Effect of Sample Injection Volume

It is obvious that the choice of sample volume is a powerful mean of varying the dispersion of the flow system. The influence of sample volume to the peak height and the corresponding dispersion was investigated by injecting various sample volumes of 30 ppm standard silicon solution into the carrier stream at the flow of 5.0 mL min^{-1}. The resulting curves are shown in Figure 3.37 and by plotting the peak height against injection volume as shown in Figure 3.38, a straight line was obtained. Therefore, an increase of the sample injection volume leads to an increase in peak height.

3.4.2.2 Effect of residence time

In addition to control the degree of dispersion of the sample zone, the residence time of sample in the system is of particular interest, as the extent of chemical conversion (formation of complex) is proportional to this factor. The flow rate of reagent stream is one parameter of interest that has effect on residence time. Figure 3.39 shows the absorbance plotted against time at various flow rates after injecting 100 uL of 30 ppm silicon standard solution and the peak height is plotted against flow rate as shown in Figure 3.40. The results from Figure 3.39 are summerized in the Table 3.16 showing the widths for base line, together with the calculated sampling rate. It is apparent that a

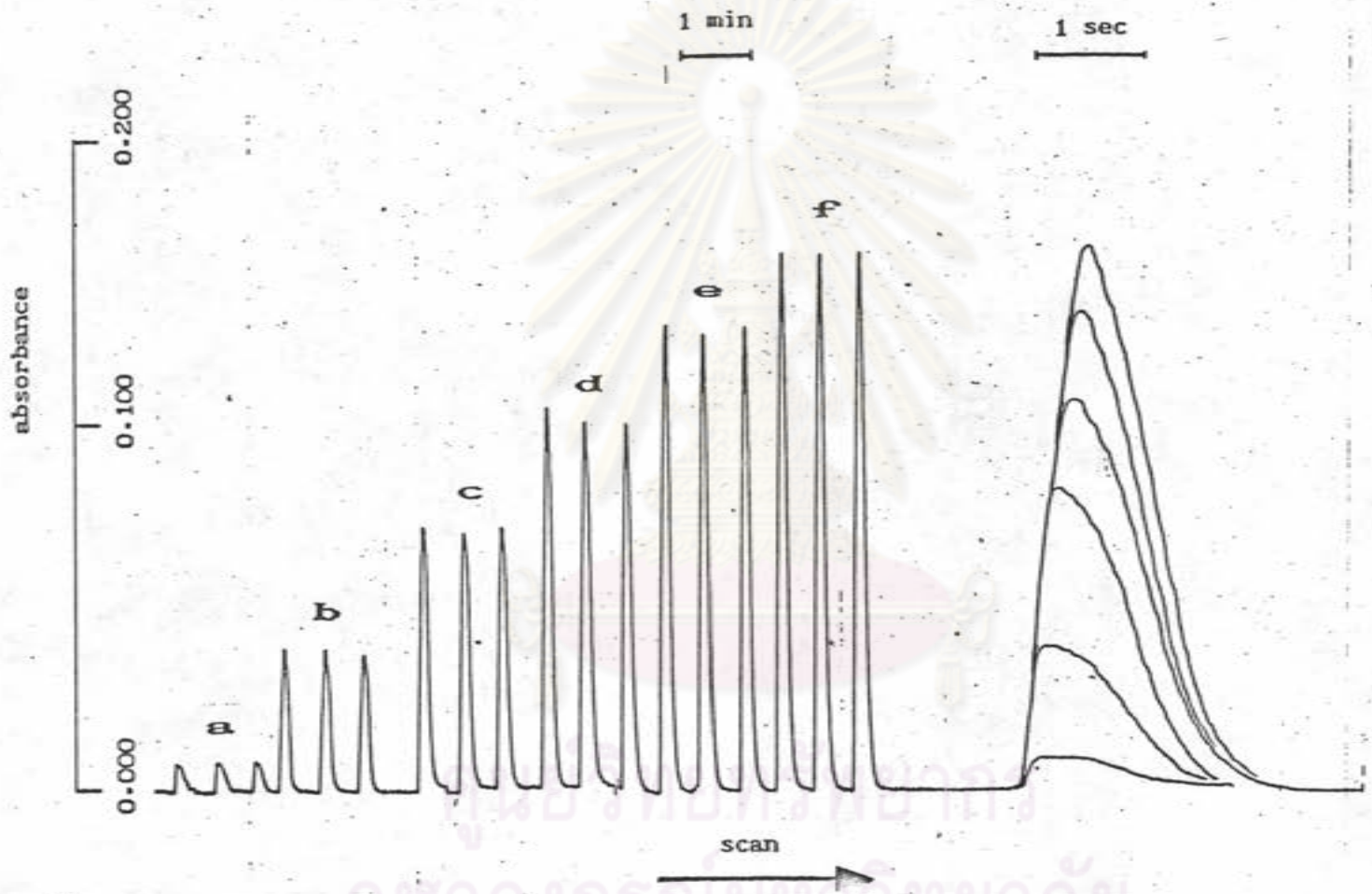

Figure 3.37 Effect of sample injection volume on sample peak for 30 ppm standard silicon solution at the flow rate of 5 mL min^{-1} by using 100 cm i.d. coil length; (a) 10, (b) 50, (c) 100, (d) 150, (e) 200 and (f) 250 ul.

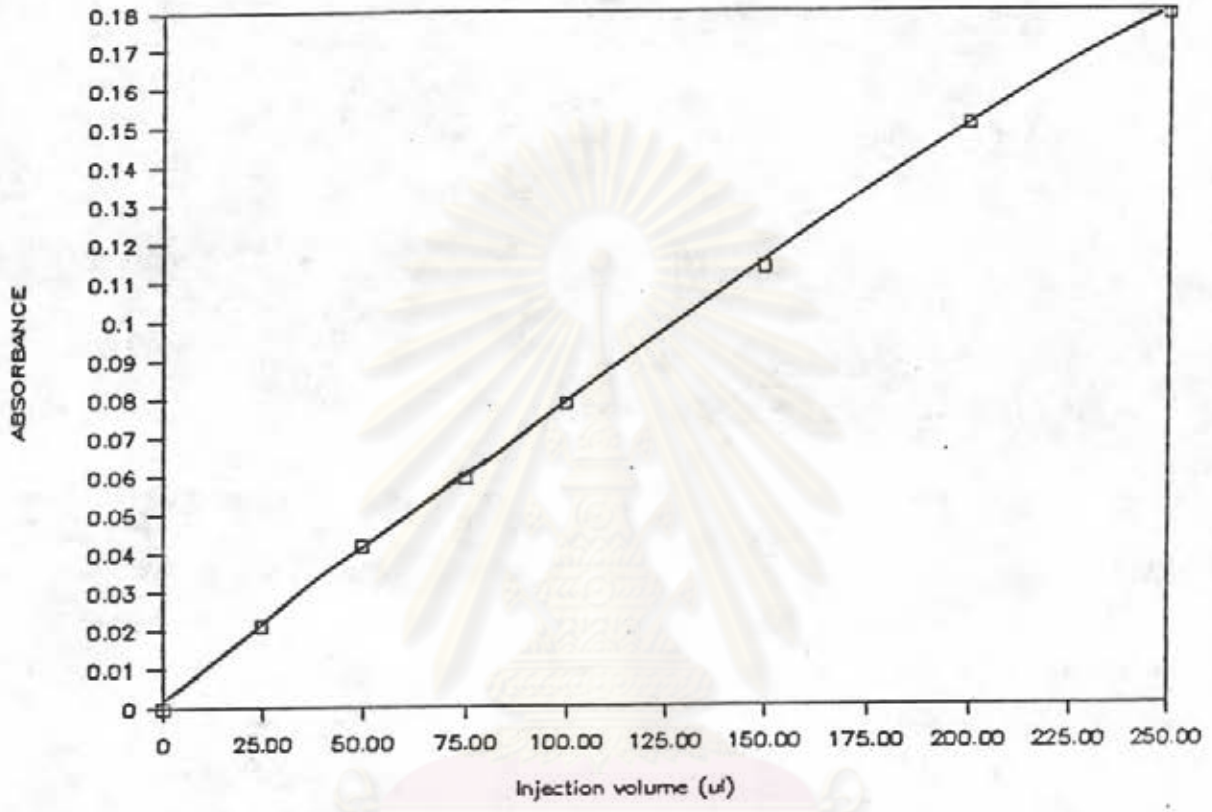

Figure 3.38 Effect of injection volume on response peaks of 30 ppm silicon injected at the flow rate of 5.0 mL min^{-1}.

decrease in the flow rate to 1.0 mL min^{-1} leads to an increase in peak height. The reason is similar to that of aluminium analysis as described in section 3.2.2.1. However, a decrease of the flow rate from 1.0 to 0.1 mL min^{-1} leads to a decrease in peak height. These effect can be expected that at this range of flow rate, the dispersion of sample zone becomes dominant. The effect of dispersion on peak tailing can also be seen in Figure 3.39 which shows that the peak is more tailing when the flow rate is decreased.

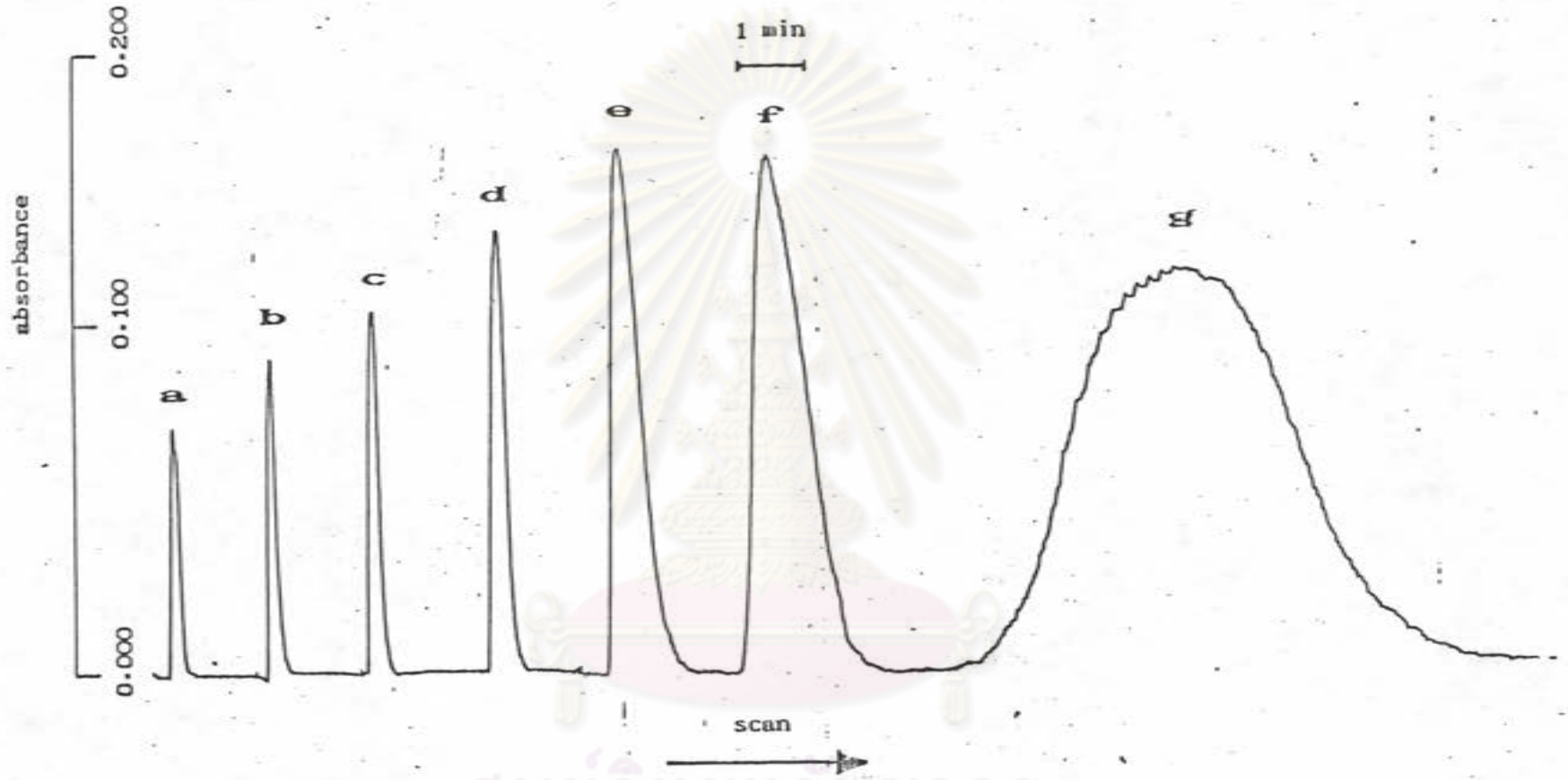

Figure 3.39 Effect of flow rate on response peaks of 100 ul 30 ppm silicon injected at various flow rate; a= 5.0, b= 4.0, c= 3.0, d=2.0, e=1.0, f= 0.5 and g= 0.1 mL min^{-1}.

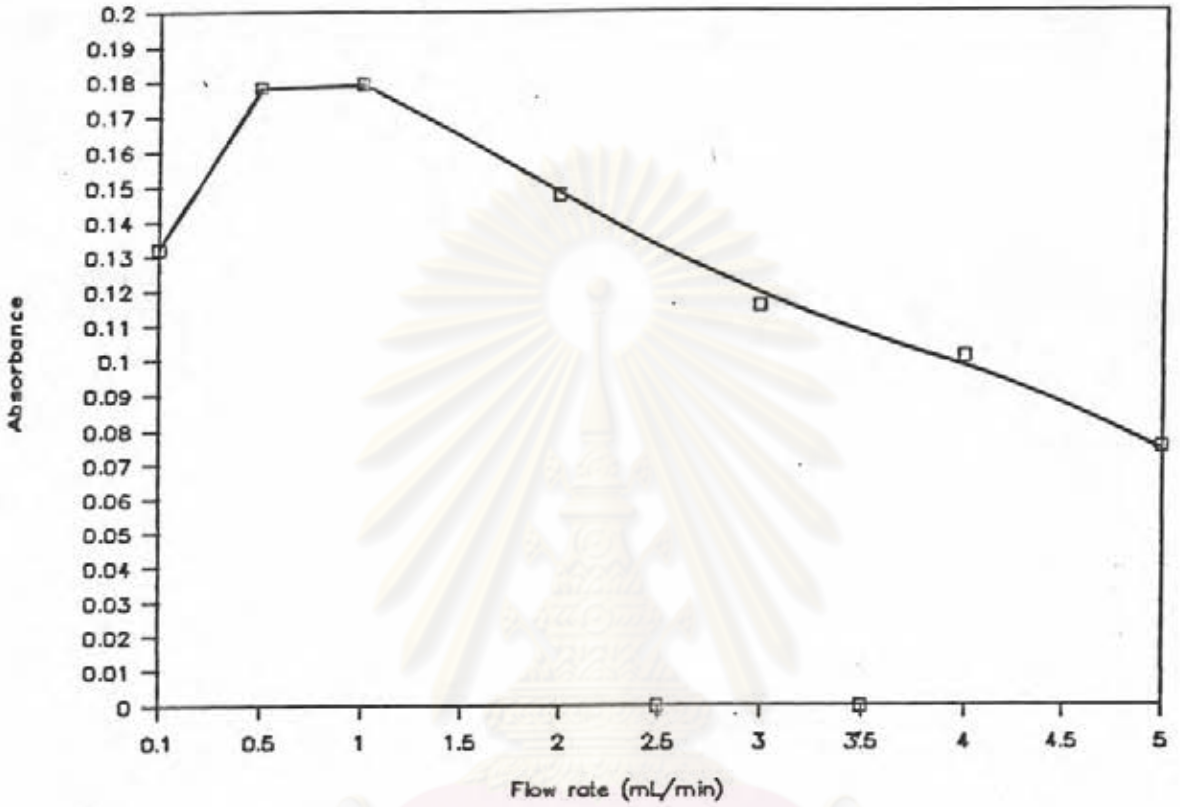

Figure 3.40 Effect of flow rate on peak heights of 100 ul 30 ppm of silicon injected at various flow rate.

The next important parameter which dispersion should be related to is the length of coil. In the study on effect of residence time on the dispersion, the mixing colis of 1.0 mm i.d. with the length of 50 to 200 cm were used. Sample peaks were recorded at various coil length as shown in Figure 3.41. The plot between the peak height and coil length in Figure 3.42 shows that an increase in coil length leads to a slightly decrease in peak height. This effect of coil length is very similar to that of pathlength or dwell time in a flow injection system decribed by Ruzicka and Hansen (22).

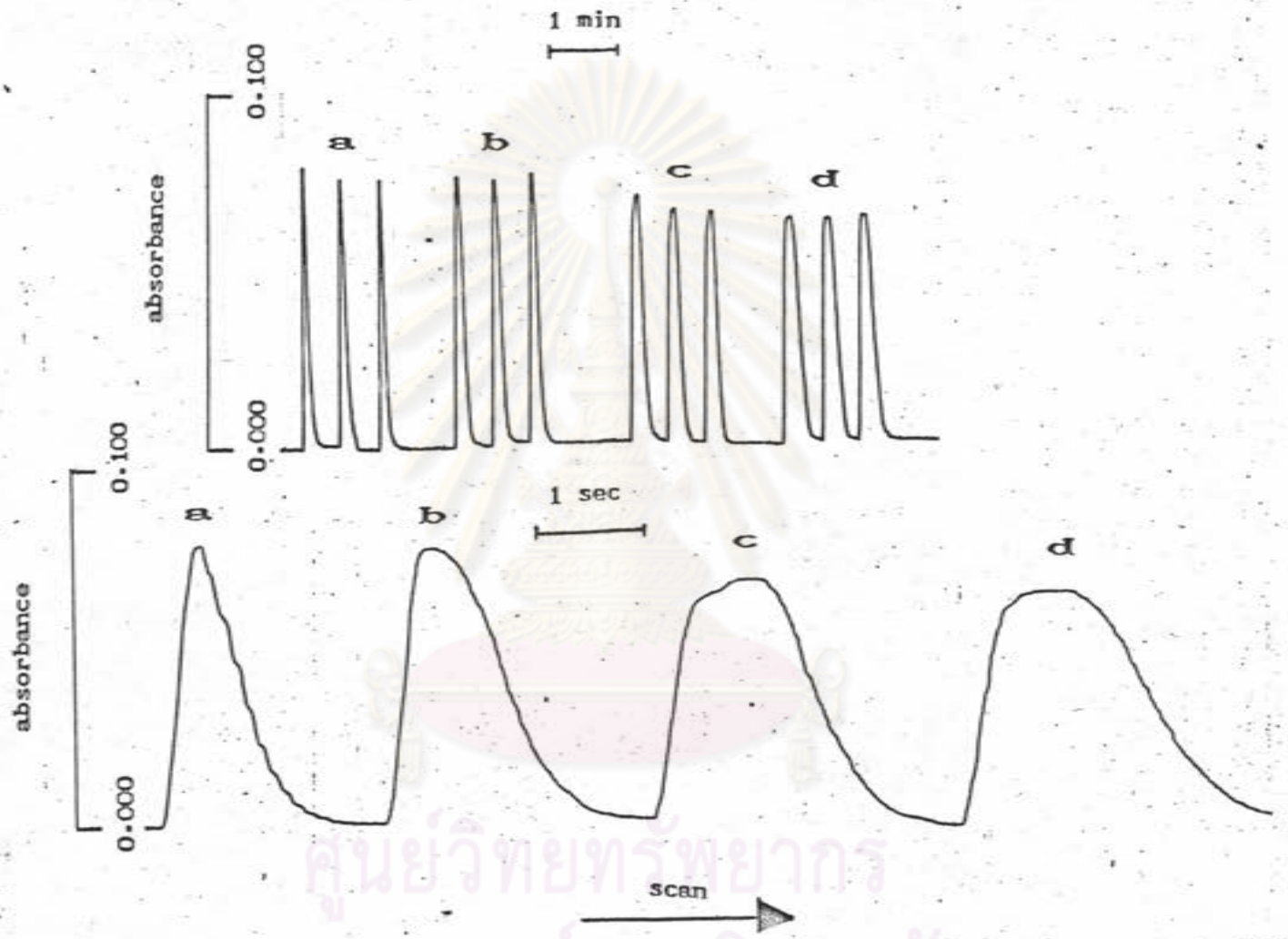

Figure 3.41 Effect of the length of 1.00 mm i.d. mixing coil on sample peak at the flow rate of 5.0 mL min^{-1}; (a) 50, (b) 100, (c) 150 and (d) 200 cm for injecting 100 uL 30 ppm standard silicon solution.

Table 3.16 Effect of flow rate on peak height, precision and sampling rate by manual injection of 100 uL of 30 ppm silicon solution at various flow rate by the use of 100 cm of 1.0 mm i.d. teflon tube.

Flow rate mL min^{-1}	Peak height Abs.	t_{base} sec	Sampling rate, h^{-1}
5.0	0.075	18	200
4.0	0.101	26	136
3.0	0.116	30	120
2.0	0.148	39	92
1.0	0.179	72	50
0.5	0.179	150	24
0.1	0.132	540	6

In the flow system, the coil diameter is one of the important parameters which effects the dispersion of system. Dispersion in flow injection analysis can be significantly reduced by using tubing of smaller diameter. In this work the coils of 0.5 and 1.0 mm i.d. were used and the result is shown in Figure 3.43. The result of this effect was unlikely to that of aluminium and iron. By injecting 100 uL of 30 ppm silicon into the carrier stream at the flow rate of 5.0 mL min^{-1} with 150 cm teflon tube, the peak height from using 0.5 mm i.d. was equal to that of 1.0 mm i.d.. Normally, the dispersion in the larger coil (1.0 mm i.d.) should be higher and will give lower peak. However, the use of the larger coil

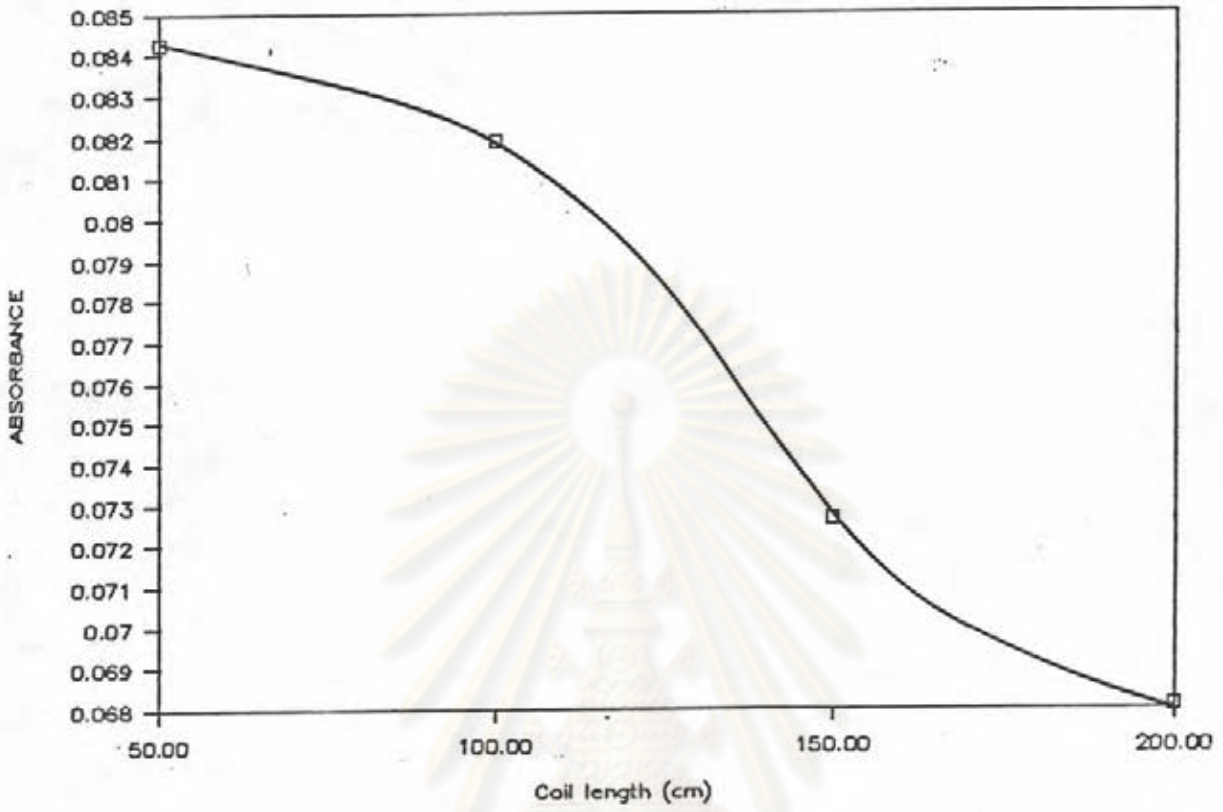

Figure 3.42 Effect of coil length on peak heights of 100 uL of 30 ppm of silicon injected at the flow rate of 5.0 mL min^{-1}.

will allow the sample and reagent to mix together much better and will also give the higher peak. This can be concluded that these two effect are nearly balanced and therefore give the nearly equal peak height.

From the study in section 3.4.2.1 and section 3.4.2.2, it can be concluded that for the determination of silicon in the flow injection system, the wavelength must be fixed at 400 nm. The optimum manifold of 50 cm with 1.0 mm i.d. tubing was employed with the flow rate of 5.0 mL min^{-1}. The study also shows that the peak

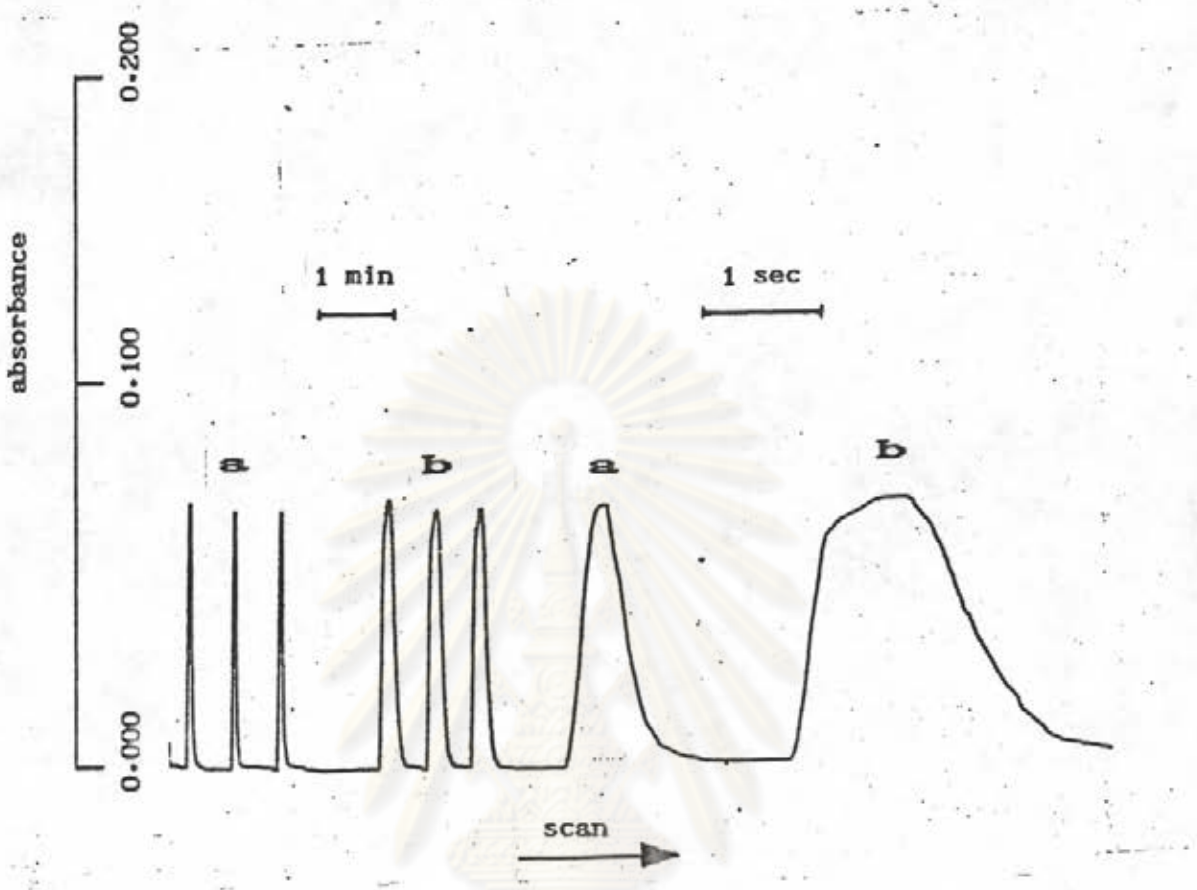

Figure 3.43 Effect of coil diameter of 150 cm coil length on sample peaks at the flow rate of 5.0 mL min^{-1}; a= 0.5 and b= 1.0 mm for 100 ul 30 ppm of standard silicon solution.

height is directly proportional to the sample injection volume. However, the sample frequency is inversely proportional to the sample injection volume. Therefore, in this work the same sample injection volume as that was used in the determination of aluminium, 75 uL, was selected.

3.4.2.3 Effect of Reagent Concentration

Reagent concentration is one parameter that effect the sensitivity of method analysis. The studies on this effect was made by using 7.50, 15.0, 22.5 and 30.0 mg/mL ammonium molybdate in 1 % sulfuric acid. The relation between the concentration of ammonium molybdate and the absorbance is shown in Figure 3.44. The sensitivity was increased with an increasing concentration of ammonium molybdate upto 15.0 mg/mL. When the reagent concentration was increased from 15.0 to 30.0 mg/mL, the sensitivity was decreased. Thus, the maximum sensitivity of the analysis can be obtained by using 15.0 mg/mL ammonium molybdate.

3.4.2.4 Effect of Sampling Rate on Reproducibility and Carry-over

The peak height reproducibility depends on several experimental factors such as the stability of reagent flow rate, an acurated injection volume, sampling rate, etc. The effect of sampling rate on peak height reproducibility is shown in Figure 3.45. The calculations of sampling rate, RSD and % CO are demonstrated in Table 3.17. The reproducibility (RSD) was decreased with the increasing sampling rate. There was no carry-over at the

sampling rate up to 120 samples h^{-1} and the reproducibility at 120 samples h^{-1} was 1.95 %.

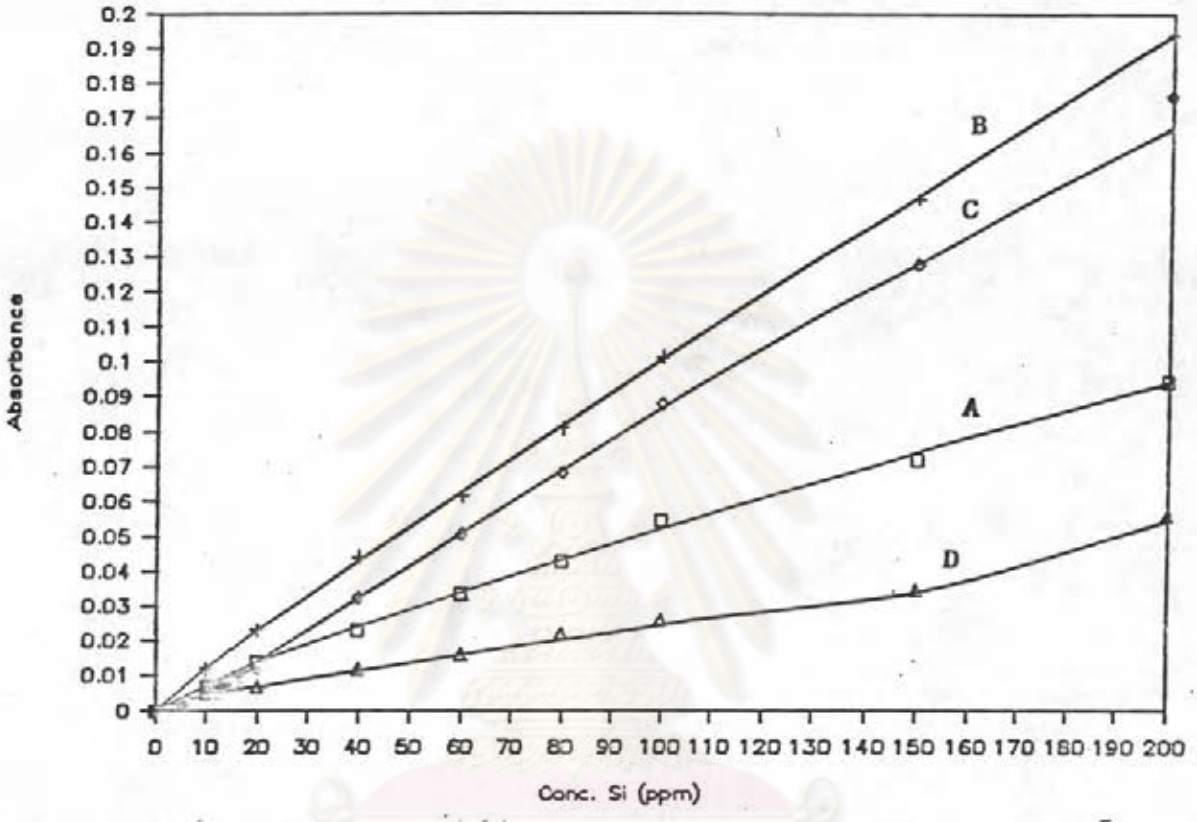

Figure 3.44 Effect of reagent concentration, A= 7.5 mg/mL; B= 15.0 mg/mL; C= 22.5 mg/mL and D= 30.0 mg/mL ammonium molybdate in 1 % sulfuric acid

3.4.2.5 Detectioc Limit and Linearity

Figure 3.46 shows the calibration plot for silicon injected into 15.0 mg/mL ammonium molybdate, using a concentration range 3.0 to 200 ppm of silicon. It was found that there was a linear relationship between the concentration of iron and absorption in the range of 5.0 to 200 ppm with the correlation coefficient of 0.999. Detection limit for this determination was 1.0 ppm.

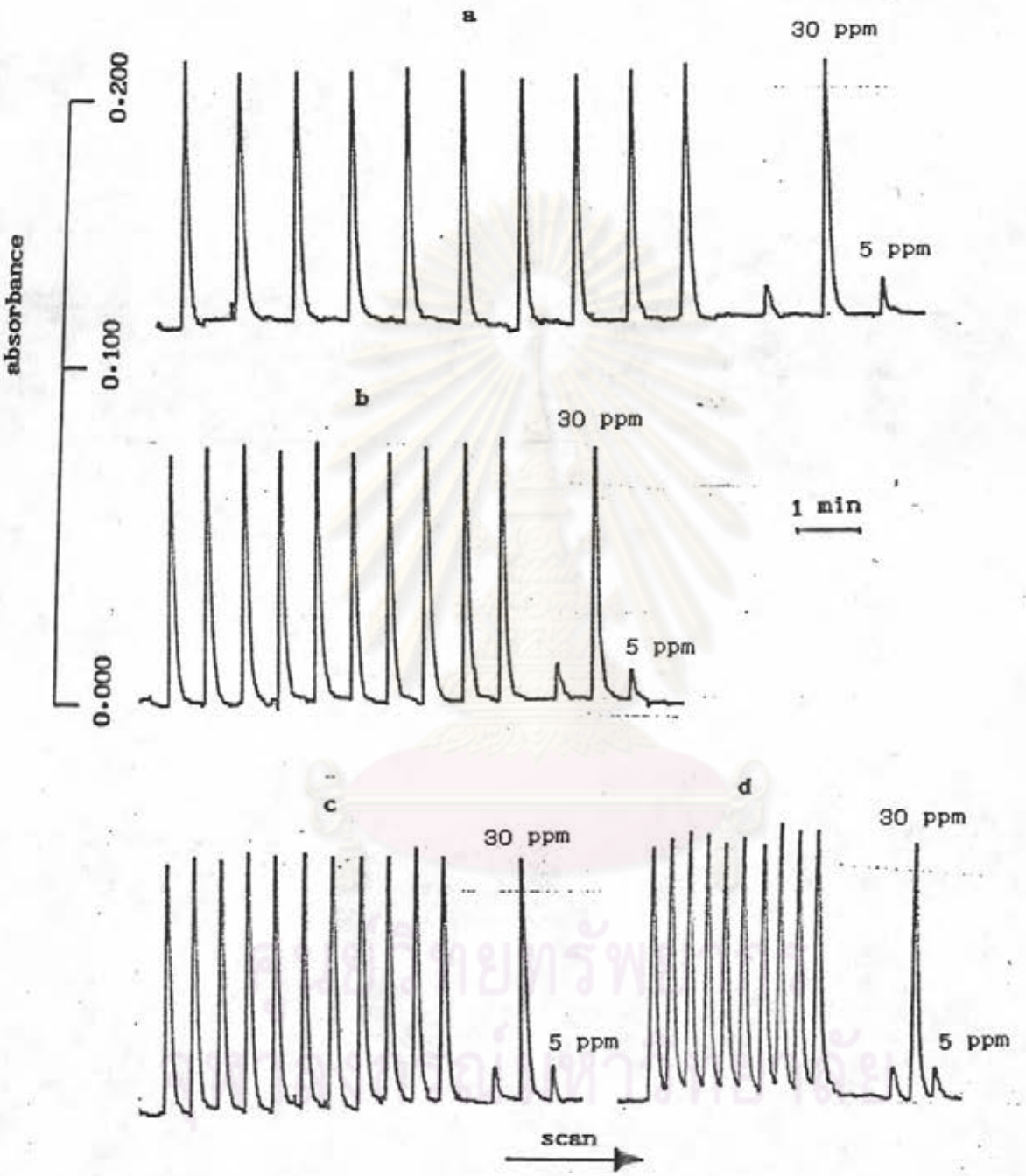

Figure 3.45 Carryover and precision of 10 replicate determinations of silicon (concentration as shown) with (a) 60, (b) 90, (c) 120 and (d) 180 samples h^{-1}.

Table 3.17 Effect of sampling rate on reproducibility and carryover.

Sampling rate $s\ h^{-1}$	Hmax Absorbance	RSD	% Carryover
60	0.0813	0.96	0.00
90	0.0827	1.14	0.00
120	0.0812	1.95	0.00
180	0.0853	2.51	2.40

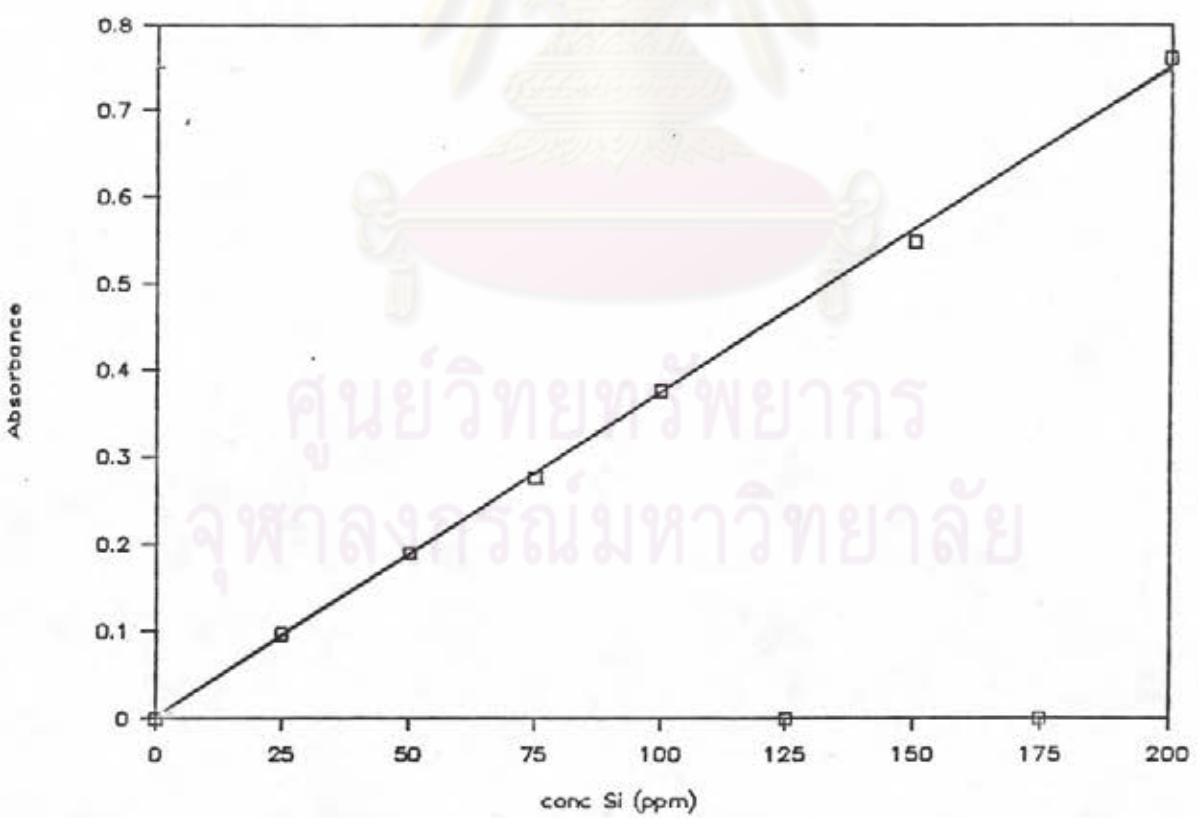

Figure 3.46 Calibration plot for silicon

3.4.2.6 Interference

The similar interference study as in the section 3.2.2.6 was carried out by using standard solution containing 100 ppm of silicon. The effect of ions on this determination is summerized in Table 3.18 which shows that barium, calcium, cobalt, copper, lithium, magnesium, potassium, zinc and nitrate do not interfere the determination of 100 ppm silicon even the concentration of these elements in the sample solution is as high as 200 ppm. Aluminium at the concentration from 150 ppm and iron at the concentration from 80 ppm will increase the peak height of the detector response. However, these effect can be deminished by precipitating these ions into the metal hydroxide with sodium hydroxide and then the precipitate is filtered offwith a filter paper. Phosphate at the concentration from 30 ppm has effect on the recorded peak by increasing the peak height. There was a report on the use of oxalic acid, citric acid, and tartaric acid (43) as masking agent for phosphate ion. In this thesis, an affect to mask phosphate by using citric acid, oxalic acid and tartaric acid is shown in Figure 3.47 which demonstrates that these reagents were inadequate for this purpose as citric acid, oxalic acid and tartaric acid were used to decompose the phosphomolybdic acid. Therefore, these reagents can protect the effect of phosphate in batch analysis but not in the flow injection system due to limitation in time. The percentage of phosphate and manganese in soil especially kaolin is found to be small when comparing with the percentage of silicon. Consequently, a masking agent for phosphate and manganese is not necessary. However, amount of phosphate is reduced in the sample preparation step. During a soil sample is fused with sodium hydroxide and dissolving the cake in 1:1 HCl, there are some

precipitation of phosphate occured in the form of zirconium phosphate which is then filtered off.

Table 3.16 Effect of cations and anions on the determination of 100 ppm silicon.

ions	Added as	maximun added without interference, ppm
aluminium	$AlCl_3$	150
barium	$BaCl_2$	200
calcium	$CaCl_2$	200
cobalt	$Co(NO_3)_2$	200
copper	$Cu(SO_4)_2$	200
iron(III)	$FeCl_3$	80
lithium	LiCl	200
magnesium	$Mg(NO_3)_2$	200
manganese	$MnSO_4$	25
potassium	KCl	200
zinc	$Zn(NO_3)_2$	200
nitrate	KNO_3	200
phosphate	$(NH_4)HPO_4$	30

3.4.3 Determination of silicon in kaolins and lateritic soils.

Table 3.19 shows the results of the determination of silicon in the synthetic kaolins and the lateritic soils by the flow

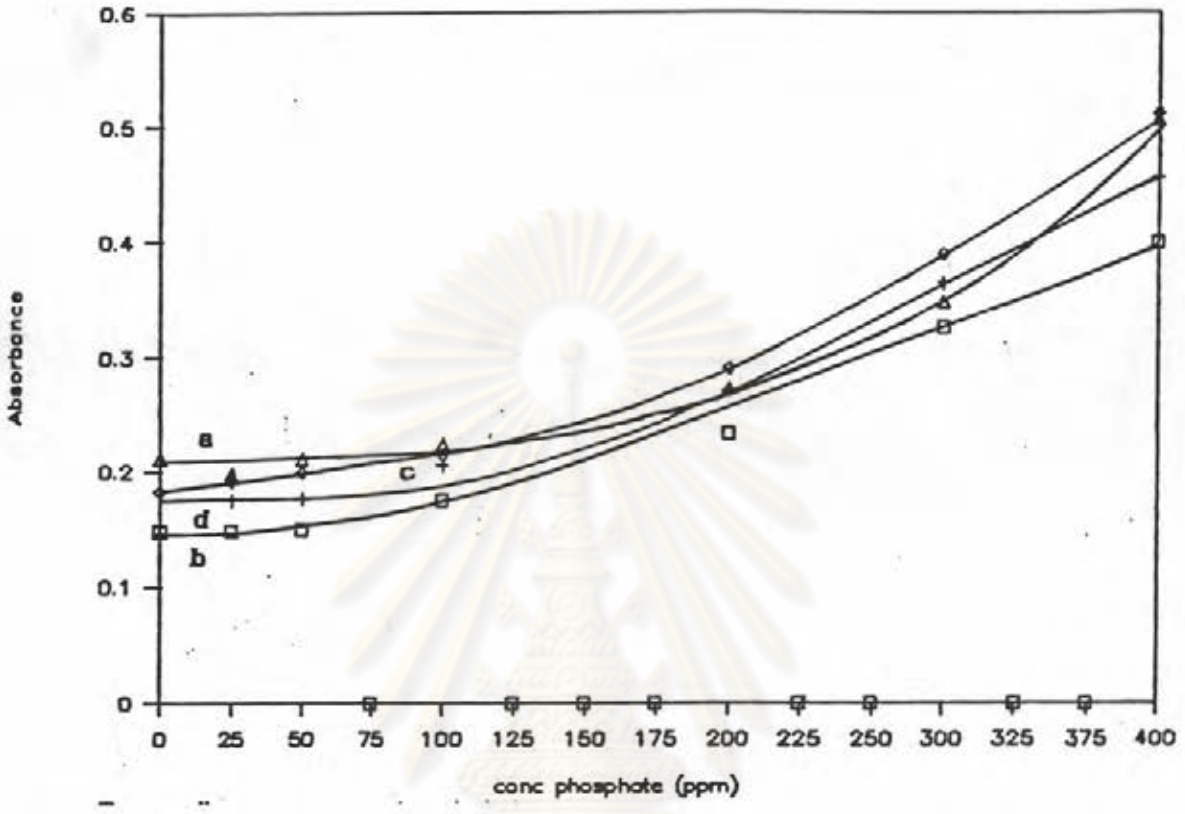

Figure 3.47 Effectiveness of phosphate to the determination of silicon (a) and the protection by using oxalic acid (b), citric acid (c) and tartaric acid (d).

injection method comparing with the classical method. From these results it can be concluded that the flow injection method gives lower percent error than the classical method. In the analysis of silica (50.0 %) in synthetic kaolin, percent recovery by the flow injection method is 99.64 % and by the classical method is 97.48 %. The results in Table 3.19 show that the determination of silica in kaolin by the classical method gives the percent recovery lower than the flow injection method. In the classical method, after the silicon was formed as silica, the precipitation of silica must be washed and filtered off for the further determination. There was some lost of

silicon from its solubility through the filtration. Therefore, the percent recovery of silicon in kaolins was lower than that of the

Table 3.19 The determination of silicon in synthetic samples by flow injection system and classical method.

Samples	Flow Injection Analysis				Classical method			
	$\%SiO_2$ w/w	%Error	RSD	%Recovery w/w	$\%SiO_2$ w/w	%Error	RSD	%Recovery w/w
Synthetic kaolin (50.0 %)	49.82	0.36	1.02	99.64	48.74	2.52	1.92	97.48
Synthetic lateritic soil(35.0 %)	34.94	0.17	1.21	99.83	35.10	0.28	0.98	100.28

flow injection analysis method. The results of silica determination in various kaolins and lateritic soils in Thailand are shown in Table 3.20. In the analysis of kaolins, percentage of silica which determined by the flow injection analysis was higher than that of the classical method. Precision (RSD) by the flow injection method is about one percent while the classical method is greater than one per cent. In the samples of lateritic soils, the results on percentage of silica by both method are in good agreement. The precision by the flow injection method is about one percent while the precision by the classical method has the lowest value at 0.76 % and the highest value at 2.68 %.

Table 3.20 Comparison of procedures for the determination of total silica in Kaolins and Lateritic soils.

Sample code	Flow Injection Analysis		Classical analysis	
	% SiO_2 (% W/W)	% RSD	% SiO_2 (% W/W)	% RSD
K-VP	47.21	1.02	46.03	1.34
K-JD	44.01	0.98	43.19	1.45
K-KM	48.41	1.14	47.63	1.99
K-PK	44.35	0.95	43.95	1.81
L-CR	43.32	1.15	43.24	0.85
L-KC	19.21	1.07	19.31	1.29
L-NK	38.01	1.28	37.92	2.68
L-UD	22.48	0.97	22.50	0.76